

## FEATURES

- **Simultaneous 50Hz/60Hz Rejection (87dB Minimum)**
- **Differential Input and Differential Reference with GND to  $V_{CC}$  Common Mode Range**
- **2ppm INL and No Missing Codes at 24 Bits**
- **0.1ppm Offset and 2.5ppm Full-Scale Error**
- **0.16ppm Noise**
- **No Latency: Digital Filter Settles in a Single Cycle.**
- Internal Oscillator—No External Components Required
- 24-Bit ADC in Narrow SSOP-16 Package (SO-8 Footprint)
- Single Supply 2.7V to 5.5V Operation
- Low Supply Current (200 $\mu$ A) and Auto Shutdown
- Pin Compatible with LTC2410

## APPLICATIONS

- Direct Sensor Digitizer
- Weight Scales
- Direct Temperature Measurement
- Gas Analyzers
- Strain-Gauge Transducers
- Instrumentation
- Data Acquisition
- Industrial Process Control
- 6-Digit DVMs
- Products for International Markets

## DESCRIPTION

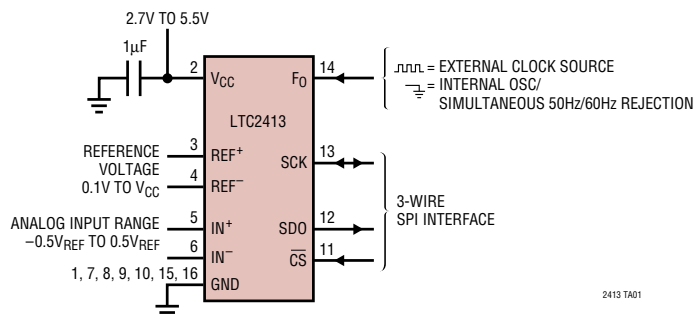
The LTC<sup>®</sup>2413 is a 2.7V to 5.5V simultaneous 50Hz/60Hz rejection micropower 24-bit differential  $\Delta\Sigma$  analog to digital converter with an integrated oscillator, 2ppm INL and 0.16ppm RMS noise. It uses delta-sigma technology and provides single cycle settling time for multiplexed applications. Through a single pin, the LTC2413 can be configured for better than 87dB input differential mode rejection over the range of 49Hz to 61.2Hz (50Hz and 60Hz  $\pm$ 2% simultaneously), or it can be driven by an external oscillator for a user defined rejection frequency. The internal oscillator requires no external frequency setting components.

The converter accepts any external differential reference voltage from 0.1V to  $V_{CC}$  for flexible ratiometric and remote sensing measurement configurations. The full-scale differential input range is from  $-0.5V_{REF}$  to  $0.5V_{REF}$ . The reference common mode voltage,  $V_{REFCM}$ , and the input common mode voltage,  $V_{INCM}$ , may be independently set anywhere within the GND to  $V_{CC}$  range of the LTC2413. The DC common mode input rejection is better than 140dB.

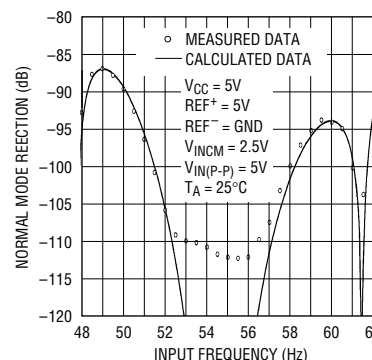
The LTC2413 communicates through a flexible 3-wire digital interface which is compatible with SPI and MICROWIRE<sup>™</sup> protocols.

**LT**, LTC and LT are registered trademarks of Linear Technology Corporation.  
 No Latency  $\Delta\Sigma$  is a trademark of Linear Technology Corporation.  
 MICROWIRE is a trademark of National Semiconductor Corporation.

## TYPICAL APPLICATION



Measured Noise Rejection from 48Hz to 62.5Hz



## ABSOLUTE MAXIMUM RATINGS

(Notes 1, 2)

Supply Voltage ( $V_{CC}$ ) to GND .....	-0.3V to 7V
Analog Input Pins Voltage to GND .....	-0.3V to ( $V_{CC} + 0.3V$ )
Reference Input Pins Voltage to GND .....	-0.3V to ( $V_{CC} + 0.3V$ )
Digital Input Voltage to GND .....	-0.3V to ( $V_{CC} + 0.3V$ )
Digital Output Voltage to GND .....	-0.3V to ( $V_{CC} + 0.3V$ )
Operating Temperature Range	
LTC2413C .....	0°C to 70°C
LTC2413I .....	-40°C to 85°C
Storage Temperature Range .....	-65°C to 150°C
Lead Temperature (Soldering, 10 sec) .....	300°C

## PACKAGE/ORDER INFORMATION

<p>TOP VIEW</p> <p>GN PACKAGE 16-LEAD PLASTIC SSOP</p> <p><math>T_{JMAX} = 125^{\circ}C</math>, <math>\theta_{JA} = 95^{\circ}C/W</math></p>	ORDER PART NUMBER
	LTC2413CGN LTC2413IGN
	GN PART MARKING
	2413 2413I

Consult factory for parts specified with wider operating temperature ranges.

## ELECTRICAL CHARACTERISTICS

The ● denotes specifications which apply over the full operating temperature range, otherwise specifications are at  $T_A = 25^{\circ}C$ . (Notes 3, 4)

PARAMETER	CONDITIONS	MIN	TYP	MAX	UNITS
Resolution (No Missing Codes)	$0.1V \leq V_{REF} \leq V_{CC}$ , $-0.5 \cdot V_{REF} \leq V_{IN} \leq 0.5 \cdot V_{REF}$ , (Note 5)	●	24		Bits
Integral Nonlinearity	$4.5V \leq V_{CC} \leq 5.5V$ , $REF^+ = 2.5V$ , $REF^- = GND$ , $V_{INCM} = 1.25V$ , (Note 6) $5V \leq V_{CC} \leq 5.5V$ , $REF^+ = 5V$ , $REF^- = GND$ , $V_{INCM} = 2.5V$ , (Note 6) $REF^+ = 2.5V$ , $REF^- = GND$ , $V_{INCM} = 1.25V$ , (Note 6)	●	1		ppm of $V_{REF}$
		●	2	14	ppm of $V_{REF}$
		●	5		ppm of $V_{REF}$
Offset Error	$2.5V \leq REF^+ \leq V_{CC}$ , $REF^- = GND$ , $GND \leq IN^+ = IN^- \leq V_{CC}$ , (Note 13)	●	0.5	2.5	$\mu V$
Offset Error Drift	$2.5V \leq REF^+ \leq V_{CC}$ , $REF^- = GND$ , $GND \leq IN^+ = IN^- \leq V_{CC}$		10		nV/ $^{\circ}C$
Positive Full-Scale Error	$2.5V \leq REF^+ \leq V_{CC}$ , $REF^- = GND$ , $IN^+ = 0.75 \cdot REF^+$ , $IN^- = 0.25 \cdot REF^+$	●	2.5	12	ppm of $V_{REF}$
Positive Full-Scale Error Drift	$2.5V \leq REF^+ \leq V_{CC}$ , $REF^- = GND$ , $IN^+ = 0.75 \cdot REF^+$ , $IN^- = 0.25 \cdot REF^+$		0.03		ppm of $V_{REF}/^{\circ}C$
Negative Full-Scale Error	$2.5V \leq REF^+ \leq V_{CC}$ , $REF^- = GND$ , $IN^+ = 0.25 \cdot REF^+$ , $IN^- = 0.75 \cdot REF^+$	●	2.5	12	ppm of $V_{REF}$
Negative Full-Scale Error Drift	$2.5V \leq REF^+ \leq V_{CC}$ , $REF^- = GND$ , $IN^+ = 0.25 \cdot REF^+$ , $IN^- = 0.75 \cdot REF^+$		0.03		ppm of $V_{REF}/^{\circ}C$
Total Unadjusted Error	$4.5V \leq V_{CC} \leq 5.5V$ , $REF^+ = 2.5V$ , $REF^- = GND$ , $V_{INCM} = 1.25V$ $5V \leq V_{CC} \leq 5.5V$ , $REF^+ = 5V$ , $REF^- = GND$ , $V_{INCM} = 2.5V$ $REF^+ = 2.5V$ , $REF^- = GND$ , $V_{INCM} = 1.25V$		3		ppm of $V_{REF}$
			3		ppm of $V_{REF}$
			4		ppm of $V_{REF}$
Output Noise	$5V \leq V_{CC} \leq 5.5V$ , $REF^+ = 5V$ , $V_{REF^-} = GND$ , $GND \leq IN^- = IN^+ \leq 5V$ , (Note 12)		0.8		$\mu V_{RMS}$

## CONVERTER CHARACTERISTICS

The ● denotes specifications which apply over the full operating temperature range, otherwise specifications are at  $T_A = 25^\circ\text{C}$ . (Notes 3, 4)

PARAMETER	CONDITIONS		MIN	TYP	MAX	UNITS
Input Common Mode Rejection DC	$2.5\text{V} \leq \text{REF}^+ \leq V_{\text{CC}}$ , $\text{REF}^- = \text{GND}$ , $\text{GND} \leq \text{IN}^- = \text{IN}^+ \leq V_{\text{CC}}$	●	130	140		dB
Input Common Mode Rejection 49Hz to 61.2Hz	$2.5\text{V} \leq \text{REF}^+ \leq V_{\text{CC}}$ , $\text{REF}^- = \text{GND}$ , $\text{GND} \leq \text{IN}^- = \text{IN}^+ \leq V_{\text{CC}}$ , (Note 7)	●	140			dB
Input Normal Mode Rejection 49Hz to 61.2Hz	(Note 7)	●	87			dB
Input Normal Mode Rejection External Clock $f_{\text{EOSC}}/2560 \pm 14\%$	External Oscillator	●	87			dB
Input Normal Mode Rejection External Clock $f_{\text{EOSC}}/2560 \pm 4\%$	External Oscillator	●	110	140		dB
Reference Common Mode Rejection DC	$2.5\text{V} \leq \text{REF}^+ \leq V_{\text{CC}}$ , $\text{GND} \leq \text{REF}^- \leq 2.5\text{V}$ , $V_{\text{REF}} = 2.5\text{V}$ , $\text{IN}^- = \text{IN}^+ = \text{GND}$	●	130	140		dB
Power Supply Rejection, DC	$\text{REF}^+ = 2.5\text{V}$ , $\text{REF}^- = \text{GND}$ , $\text{IN}^- = \text{IN}^+ = \text{GND}$			120		dB
Power Supply Rejection Simultaneous 50Hz/60Hz $\pm 2\%$	$\text{REF}^+ = 2.5\text{V}$ , $\text{REF}^- = \text{GND}$ , $\text{IN}^- = \text{IN}^+ = \text{GND}$ , (Note 7)			120		dB

## ANALOG INPUT AND REFERENCE

The ● denotes specifications which apply over the full operating temperature range, otherwise specifications are at  $T_A = 25^\circ\text{C}$ . (Note 3)

SYMBOL	PARAMETER	CONDITIONS		MIN	TYP	MAX	UNITS
$\text{IN}^+$	Absolute/Common Mode $\text{IN}^+$ Voltage		●	$\text{GND} - 0.3\text{V}$		$V_{\text{CC}} + 0.3\text{V}$	V
$\text{IN}^-$	Absolute/Common Mode $\text{IN}^-$ Voltage		●	$\text{GND} - 0.3\text{V}$		$V_{\text{CC}} + 0.3\text{V}$	V
$V_{\text{IN}}$	Input Differential Voltage Range ( $\text{IN}^+ - \text{IN}^-$ )		●	$-V_{\text{REF}}/2$		$V_{\text{REF}}/2$	V
$\text{REF}^+$	Absolute/Common Mode $\text{REF}^+$ Voltage		●	0.1		$V_{\text{CC}}$	V
$\text{REF}^-$	Absolute/Common Mode $\text{REF}^-$ Voltage		●	GND		$V_{\text{CC}} - 0.1\text{V}$	V
$V_{\text{REF}}$	Reference Differential Voltage Range ( $\text{REF}^+ - \text{REF}^-$ )		●	0.1		$V_{\text{CC}}$	V
$C_S (\text{IN}^+)$	$\text{IN}^+$ Sampling Capacitance				18		pF
$C_S (\text{IN}^-)$	$\text{IN}^-$ Sampling Capacitance				18		pF
$C_S (\text{REF}^+)$	$\text{REF}^+$ Sampling Capacitance				18		pF
$C_S (\text{REF}^-)$	$\text{REF}^-$ Sampling Capacitance				18		pF
$I_{\text{DC\_LEAK}} (\text{IN}^+)$	$\text{IN}^+$ DC Leakage Current	$\overline{\text{CS}} = V_{\text{CC}}$ , $\text{IN}^+ = \text{GND}$	●	-10	1	10	nA
$I_{\text{DC\_LEAK}} (\text{IN}^-)$	$\text{IN}^-$ DC Leakage Current	$\overline{\text{CS}} = V_{\text{CC}}$ , $\text{IN}^- = \text{GND}$	●	-10	1	10	nA
$I_{\text{DC\_LEAK}} (\text{REF}^+)$	$\text{REF}^+$ DC Leakage Current	$\overline{\text{CS}} = V_{\text{CC}}$ , $\text{REF}^+ = 5\text{V}$	●	-10	1	10	nA
$I_{\text{DC\_LEAK}} (\text{REF}^-)$	$\text{REF}^-$ DC Leakage Current	$\overline{\text{CS}} = V_{\text{CC}}$ , $\text{REF}^- = \text{GND}$	●	-10	1	10	nA

## DIGITAL INPUTS AND DIGITAL OUTPUTS

The ● denotes specifications which apply over the full operating temperature range, otherwise specifications are at  $T_A = 25^\circ\text{C}$ . (Note 3)

SYMBOL	PARAMETER	CONDITIONS	MIN	TYP	MAX	UNITS
$V_{IH}$	High Level Input Voltage CS, F <sub>0</sub>	$2.7V \leq V_{CC} \leq 5.5V$	●	2.5		V
		$2.7V \leq V_{CC} \leq 3.3V$		2.0		V
$V_{IL}$	Low Level Input Voltage CS, F <sub>0</sub>	$4.5V \leq V_{CC} \leq 5.5V$	●		0.8	V
		$2.7V \leq V_{CC} \leq 5.5V$			0.6	V
$V_{IH}$	High Level Input Voltage SCK	$2.7V \leq V_{CC} \leq 5.5V$ (Note 8)	●	2.5		V
		$2.7V \leq V_{CC} \leq 3.3V$ (Note 8)		2.0		V
$V_{IL}$	Low Level Input Voltage SCK	$4.5V \leq V_{CC} \leq 5.5V$ (Note 8)	●		0.8	V
		$2.7V \leq V_{CC} \leq 5.5V$ (Note 8)			0.6	V
$I_{IN}$	Digital Input Current CS, F <sub>0</sub>	$0V \leq V_{IN} \leq V_{CC}$	●	-10	10	$\mu\text{A}$
$I_{IN}$	Digital Input Current SCK	$0V \leq V_{IN} \leq V_{CC}$ (Note 8)	●	-10	10	$\mu\text{A}$
$C_{IN}$	Digital Input Capacitance CS, F <sub>0</sub>			10		pF
$C_{IN}$	Digital Input Capacitance SCK	(Note 8)		10		pF
$V_{OH}$	High Level Output Voltage SDO	$I_O = -800\mu\text{A}$	●	$V_{CC} - 0.5V$		V
$V_{OL}$	Low Level Output Voltage SDO	$I_O = 1.6\text{mA}$	●		0.4	V
$V_{OH}$	High Level Output Voltage SCK	$I_O = -800\mu\text{A}$ (Note 9)	●	$V_{CC} - 0.5V$		V
$V_{OL}$	Low Level Output Voltage SCK	$I_O = 1.6\text{mA}$ (Note 9)	●		0.4	V
$I_{OZ}$	Hi-Z Output Leakage SDO		●	-10	10	$\mu\text{A}$

## POWER REQUIREMENTS

The ● denotes specifications which apply over the full operating temperature range, otherwise specifications are at  $T_A = 25^\circ\text{C}$ . (Note 3)

SYMBOL	PARAMETER	CONDITIONS	MIN	TYP	MAX	UNITS
$V_{CC}$	Supply Voltage		●	2.7	5.5	V
$I_{CC}$	Supply Current Conversion Mode Sleep Mode	$\overline{CS} = 0V$ (Note 11)	●	200	300	$\mu\text{A}$
		$\overline{CS} = V_{CC}$ (Note 11)	●	20	30	$\mu\text{A}$

## TIMING CHARACTERISTICS

The ● denotes specifications which apply over the full operating temperature range, otherwise specifications are at  $T_A = 25^\circ\text{C}$ . (Note 3)

SYMBOL	PARAMETER	CONDITIONS	MIN	TYP	MAX	UNITS
$f_{\text{EOSC}}$	External Oscillator Frequency Range		2.56		2000	kHz
$t_{\text{HEO}}$	External Oscillator High Period		0.25		390	$\mu\text{s}$
$t_{\text{LEO}}$	External Oscillator Low Period		0.25		390	$\mu\text{s}$
$t_{\text{CONV}}$	Conversion Time	$F_0 = 0\text{V}$ External Oscillator (Note 10)		146.71 $20510/f_{\text{EOSC}}$ (in kHz)		ms ms
$f_{\text{ISCK}}$	Internal SCK Frequency	Internal Oscillator (Note 9) External Oscillator (Notes 9, 10)		17.5 $f_{\text{EOSC}}/8$		kHz kHz
$D_{\text{ISCK}}$	Internal SCK Duty Cycle	(Note 9)	45		55	%
$f_{\text{ESCK}}$	External SCK Frequency Range	(Note 8)			2000	kHz
$t_{\text{LESCK}}$	External SCK Low Period	(Note 8)	250			ns
$t_{\text{HESCK}}$	External SCK High Period	(Note 8)	250			ns
$t_{\text{DOUT\_ISCK}}$	Internal SCK 32-Bit Data Output Time	Internal Oscillator (Notes 9, 11) External Oscillator (Notes 9, 10)	1.80	1.83 $256/f_{\text{EOSC}}$ (in kHz)	1.86	ms ms
$t_{\text{DOUT\_ESCK}}$	External SCK 32-Bit Data Output Time	(Note 8)		$32/f_{\text{ESCK}}$ (in kHz)		ms
$t_1$	$\overline{\text{CS}} \downarrow$ to SDO Low Z		0		200	ns
$t_2$	$\overline{\text{CS}} \uparrow$ to SDO Hi-Z		0		200	ns
$t_3$	$\overline{\text{CS}} \downarrow$ to SCK $\downarrow$	(Note 9)	0		200	ns
$t_4$	$\overline{\text{CS}} \downarrow$ to SCK $\uparrow$	(Note 8)	50			ns
$t_{\text{KQMAX}}$	SCK $\downarrow$ to SDO Valid				220	ns
$t_{\text{KQMIN}}$	SDO Hold After SCK $\downarrow$	(Note 5)	15			ns
$t_5$	SCK Set-Up Before $\overline{\text{CS}} \downarrow$		50			ns
$t_6$	SCK Hold After $\overline{\text{CS}} \downarrow$				50	ns

**Note 1:** Absolute Maximum Ratings are those values beyond which the life of the device may be impaired.

**Note 2:** All voltage values are with respect to GND.

**Note 3:**  $V_{\text{CC}} = 2.7\text{V}$  to  $5.5\text{V}$  unless otherwise specified.

$V_{\text{REF}} = \text{REF}^+ - \text{REF}^-$ ,  $V_{\text{REFCM}} = (\text{REF}^+ + \text{REF}^-)/2$ ;

$V_{\text{IN}} = \text{IN}^+ - \text{IN}^-$ ,  $V_{\text{INCM}} = (\text{IN}^+ + \text{IN}^-)/2$ .

**Note 4:**  $F_0$  pin tied to GND or to external conversion clock source with  $f_{\text{EOSC}} = 139800\text{Hz}$  unless otherwise specified.

**Note 5:** Guaranteed by design, not subject to test.

**Note 6:** Integral nonlinearity is defined as the deviation of a code from a straight line passing through the actual endpoints of the transfer curve. The deviation is measured from the center of the quantization band.

**Note 7:**  $F_0 = 0\text{V}$  (internal oscillator) or  $f_{\text{EOSC}} = 139800\text{Hz} \pm 2\%$  (external oscillator).

**Note 8:** The converter is in external SCK mode of operation such that the SCK pin is used as digital input. The frequency of the clock signal driving SCK during the data output is  $f_{\text{ESCK}}$  and is expressed in kHz.

**Note 9:** The converter is in internal SCK mode of operation such that the SCK pin is used as digital output.

**Note 10:** The external oscillator is connected to the  $F_0$  pin. The external oscillator frequency,  $f_{\text{EOSC}}$ , is expressed in kHz.

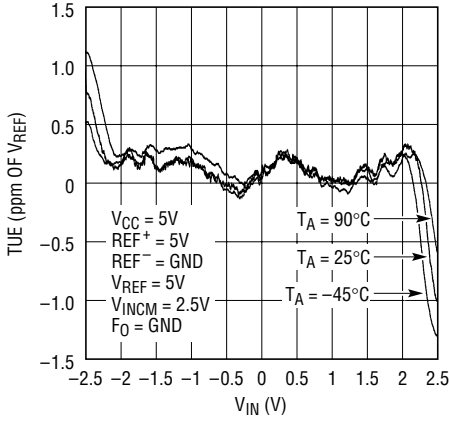
**Note 11:** The converter uses the internal oscillator.  $F_0 = 0\text{V}$ .

**Note 12:** The output noise includes the contribution of the internal calibration operations.

**Note 13:** Guaranteed by design and test correlation.

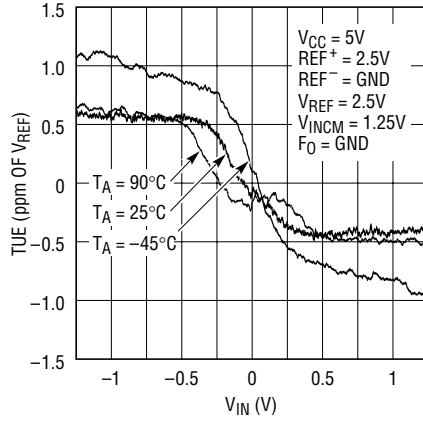
**TYPICAL PERFORMANCE CHARACTERISTICS**

**Total Unadjusted Error vs Temperature ( $V_{CC} = 5V$ ,  $V_{REF} = 5V$ )**



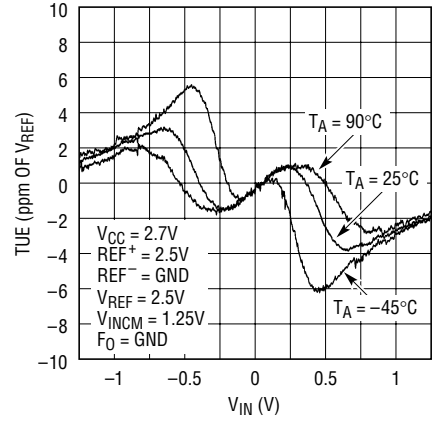
2413 G01

**Total Unadjusted Error vs Temperature ( $V_{CC} = 5V$ ,  $V_{REF} = 2.5V$ )**



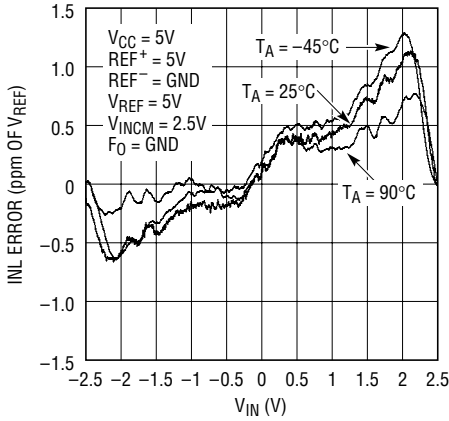
2413 G02

**Total Unadjusted Error vs Temperature ( $V_{CC} = 2.7V$ ,  $V_{REF} = 2.5V$ )**



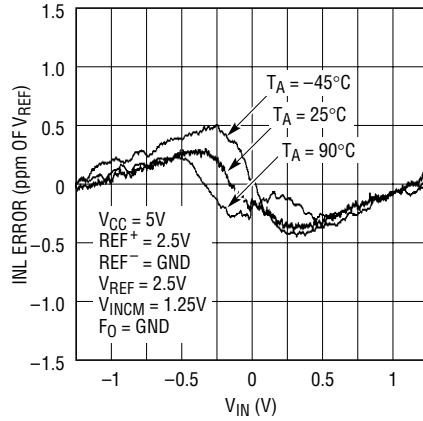
2413 G03

**Integral Nonlinearity vs Temperature ( $V_{CC} = 5V$ ,  $V_{REF} = 5V$ )**



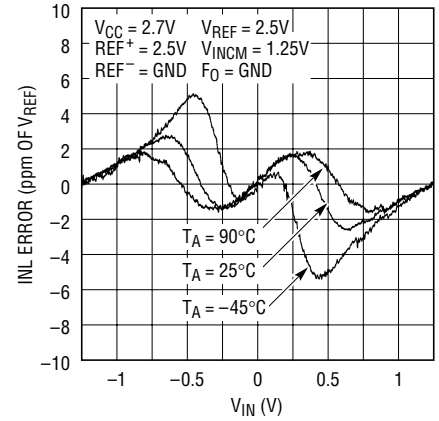
2413 G04

**Integral Nonlinearity vs Temperature ( $V_{CC} = 5V$ ,  $V_{REF} = 2.5V$ )**



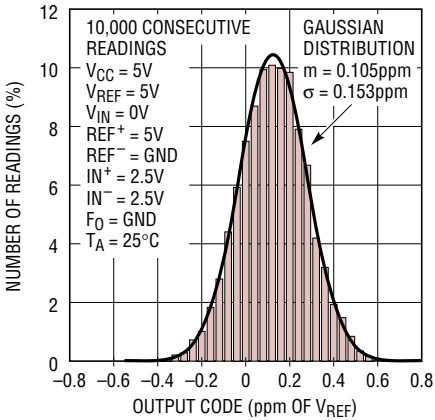
2413 G05

**Integral Nonlinearity vs Temperature ( $V_{CC} = 2.7V$ ,  $V_{REF} = 2.5V$ )**



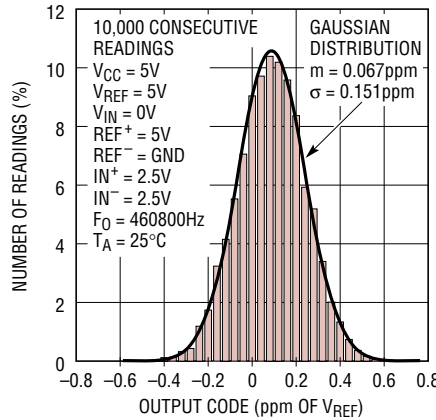
2413 G06

**Noise Histogram (Output Rate = 6.83Hz,  $V_{CC} = 5V$ ,  $V_{REF} = 5V$ )**



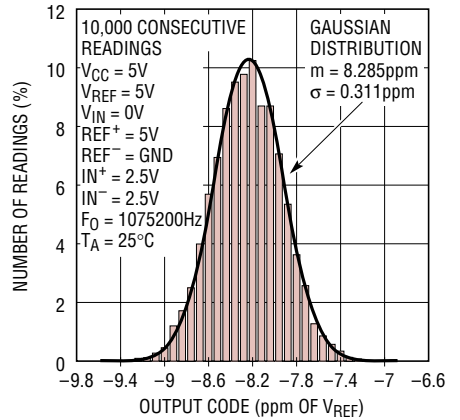
2413 G07

**Noise Histogram (Output Rate = 22.5Hz,  $V_{CC} = 5V$ ,  $V_{REF} = 5V$ )**



2413 G08

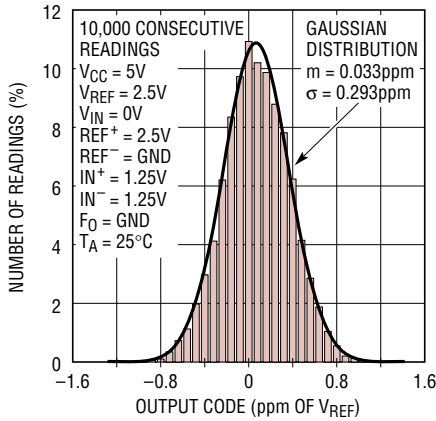
**Noise Histogram (Output Rate = 52.5Hz,  $V_{CC} = 5V$ ,  $V_{REF} = 5V$ )**



sn2413 2413fs

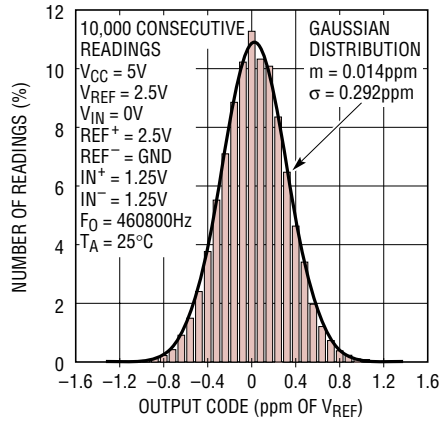
# TYPICAL PERFORMANCE CHARACTERISTICS

**Noise Histogram (Output Rate = 6.83Hz,  $V_{CC} = 5V$ ,  $V_{REF} = 2.5V$ )**



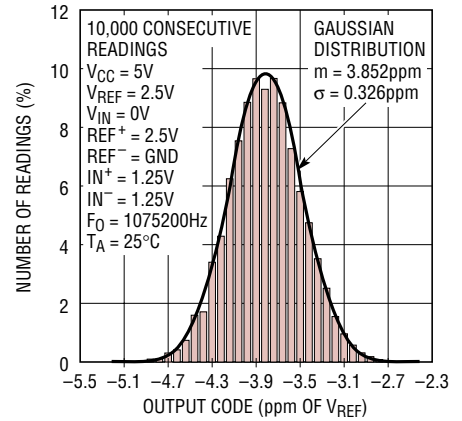
2413 G10

**Noise Histogram (Output Rate = 22.5Hz,  $V_{CC} = 5V$ ,  $V_{REF} = 2.5V$ )**



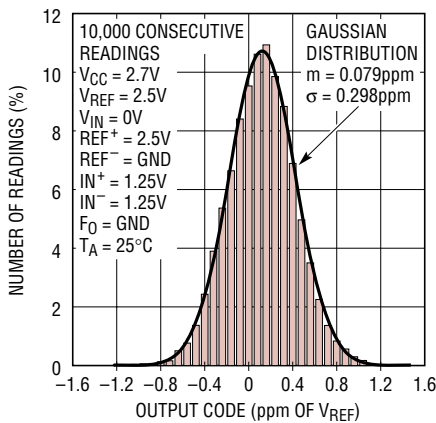
2413 G11

**Noise Histogram (Output Rate = 52.5Hz,  $V_{CC} = 5V$ ,  $V_{REF} = 2.5V$ )**



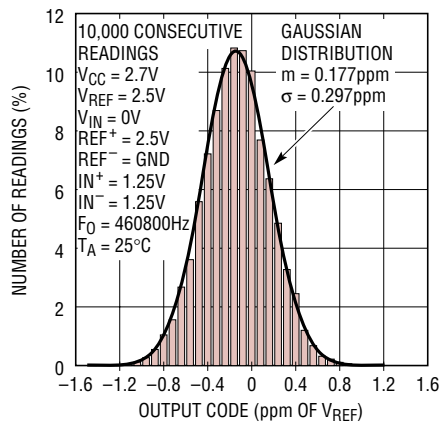
2413 G12

**Noise Histogram (Output Rate = 6.83Hz,  $V_{CC} = 2.7V$ ,  $V_{REF} = 2.5V$ )**



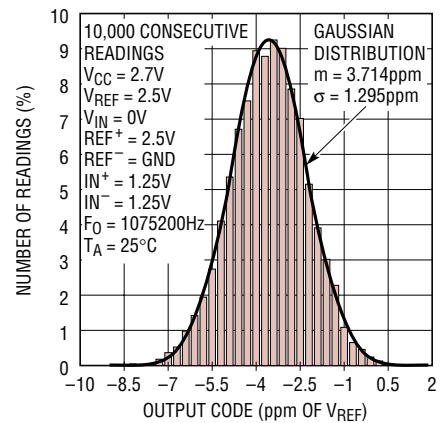
2413 G13

**Noise Histogram (Output Rate = 22.5Hz,  $V_{CC} = 2.7V$ ,  $V_{REF} = 2.5V$ )**



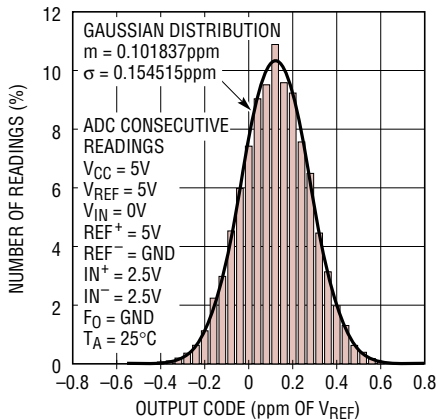
2413 G14

**Noise Histogram (Output Rate = 52.5Hz,  $V_{CC} = 2.7V$ ,  $V_{REF} = 2.5V$ )**



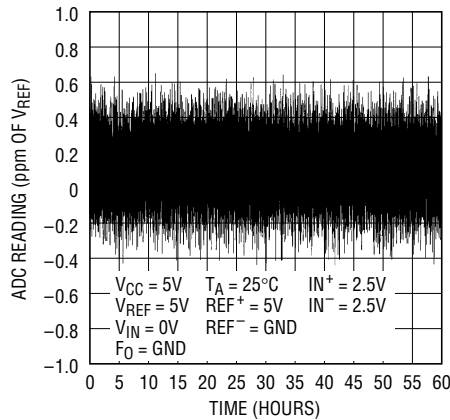
2413 G15

**Long-Term Noise Histogram (Time = 60 Hrs,  $V_{CC} = 5V$ ,  $V_{REF} = 5V$ )**



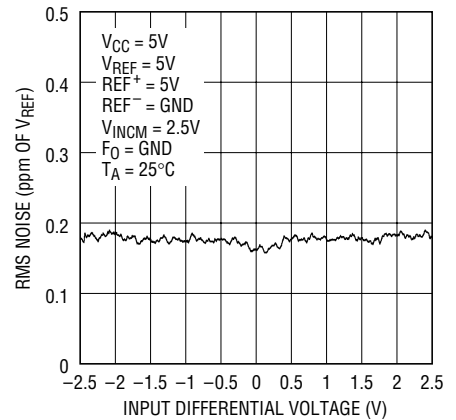
2413 G16

**Consecutive ADC Readings vs Time**



2413 G17

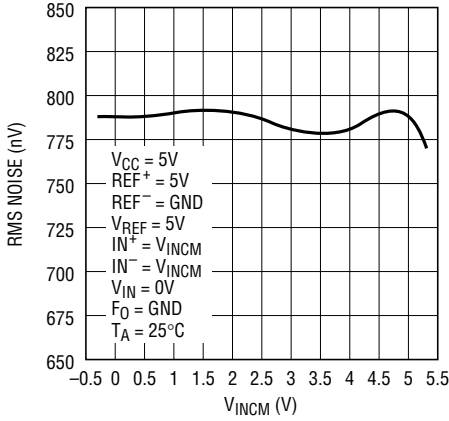
**RMS Noise vs Input Differential Voltage**



sn241312413fs

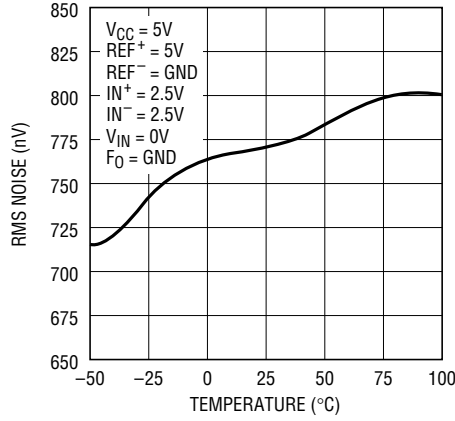
## TYPICAL PERFORMANCE CHARACTERISTICS

### RMS Noise vs $V_{INCM}$



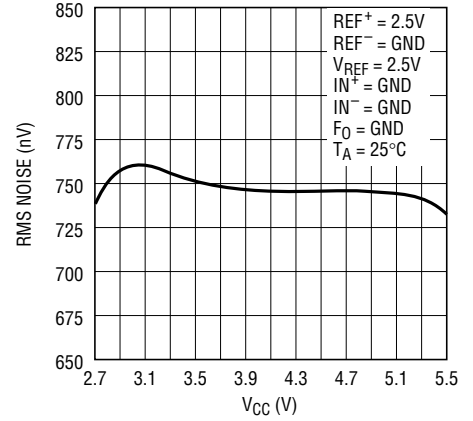
2413 G19

### RMS Noise vs Temperature ( $T_A$ )



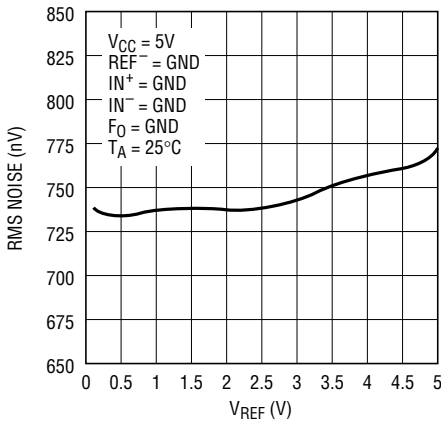
2413 G20

### RMS Noise vs $V_{CC}$



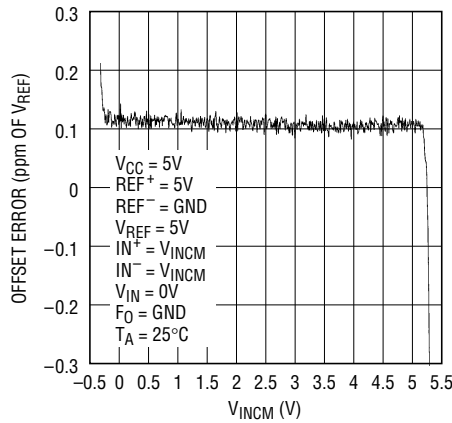
2413 G21

### RMS Noise vs $V_{REF}$



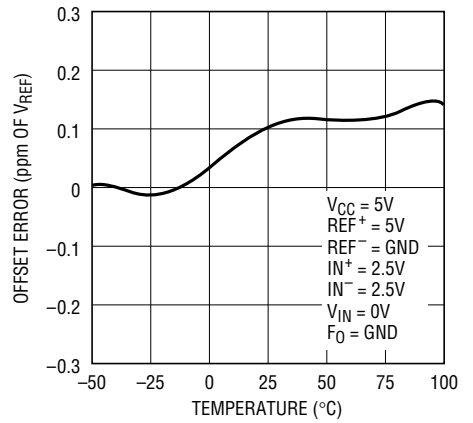
2413 G22

### Offset Error vs $V_{INCM}$



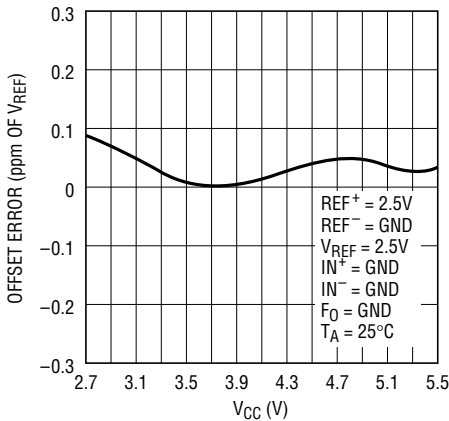
2413 G23

### Offset Error vs Temperature ( $T_A$ )



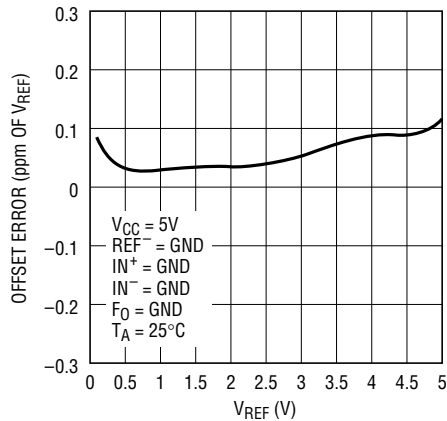
2413 G24

### Offset Error vs $V_{CC}$



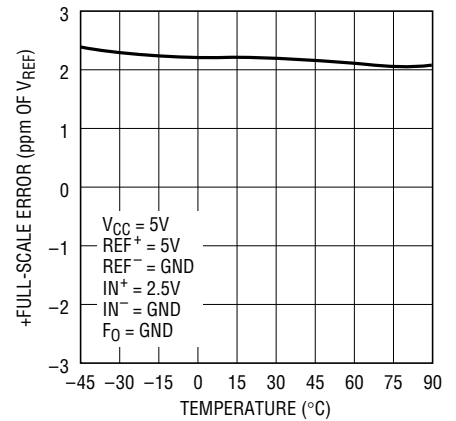
2413 G25

### Offset Error vs $V_{REF}$



2413 G26

### + Full-Scale Error vs Temperature ( $T_A$ )

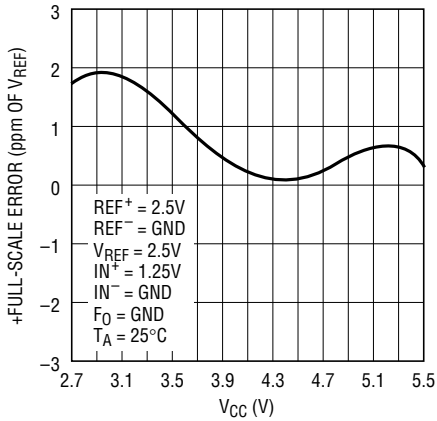


2413 G27



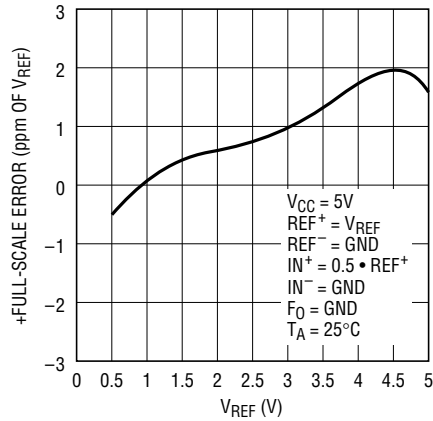
# TYPICAL PERFORMANCE CHARACTERISTICS

**+ Full-Scale Error vs  $V_{CC}$**



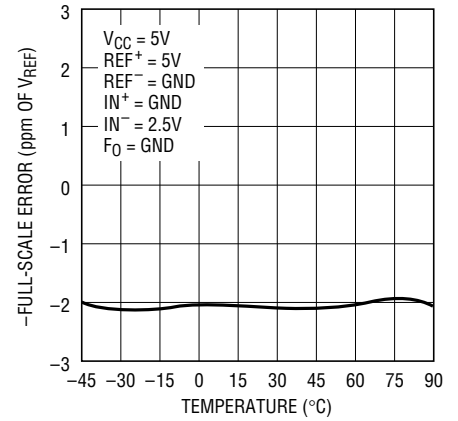
2413 G28

**+ Full-Scale Error vs  $V_{REF}$**



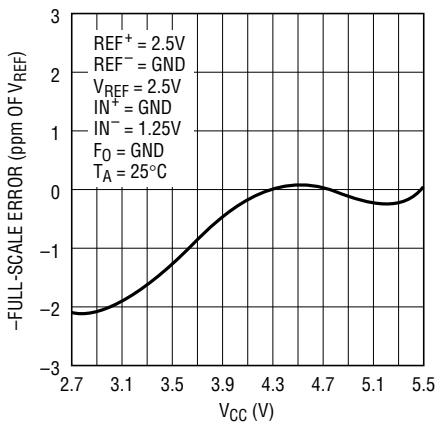
2413 G29

**- Full-Scale Error vs Temperature ( $T_A$ )**



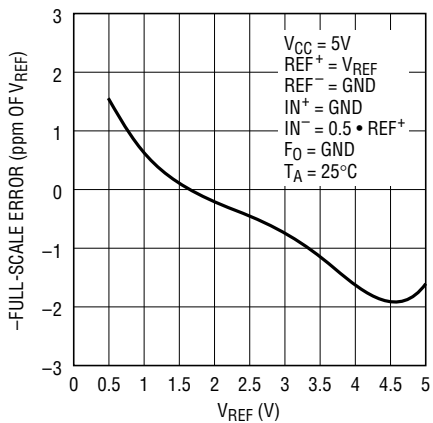
2413 G30

**- Full-Scale Error vs  $V_{CC}$**



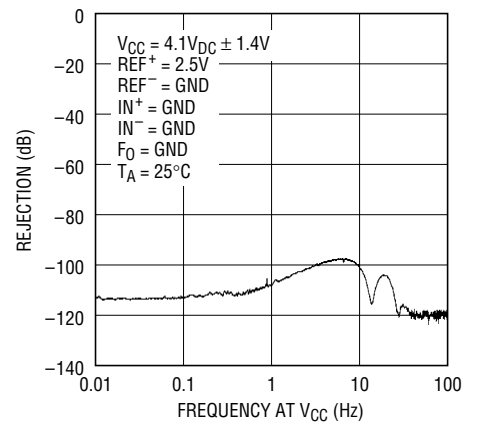
2413 G31

**- Full-Scale Error vs  $V_{REF}$**



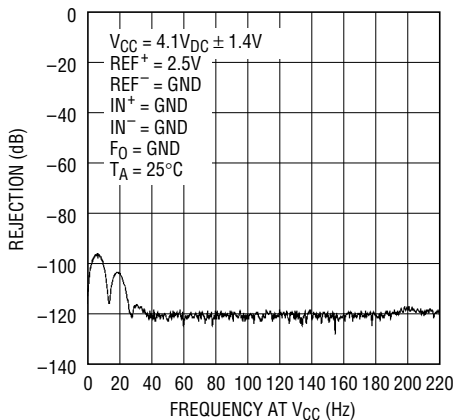
2413 G32

**PSRR vs Frequency at  $V_{CC}$**



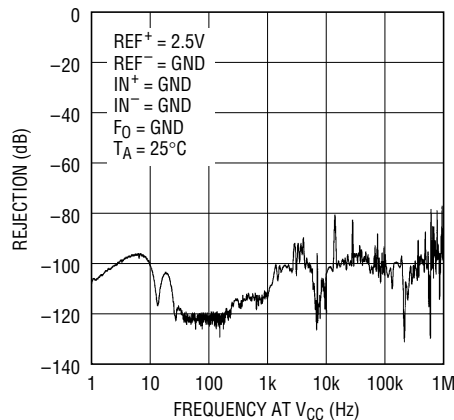
2413 G33

**PSRR vs Frequency at  $V_{CC}$**



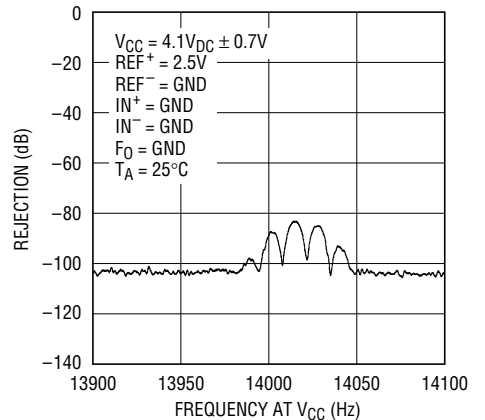
2413 G34

**PSRR vs Frequency at  $V_{CC}$**



2413 G35

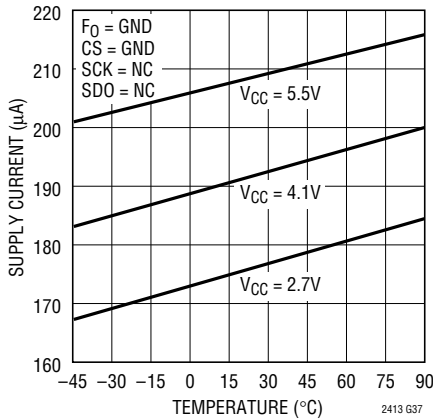
**PSRR vs Frequency at  $V_{CC}$**



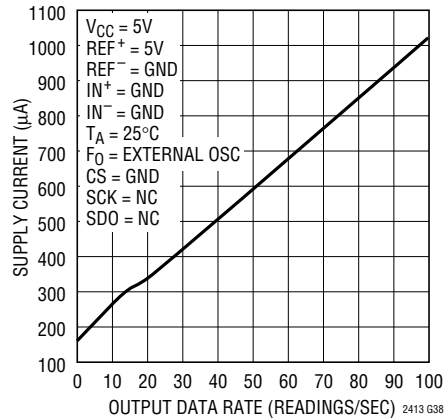
2413 G36

## TYPICAL PERFORMANCE CHARACTERISTICS

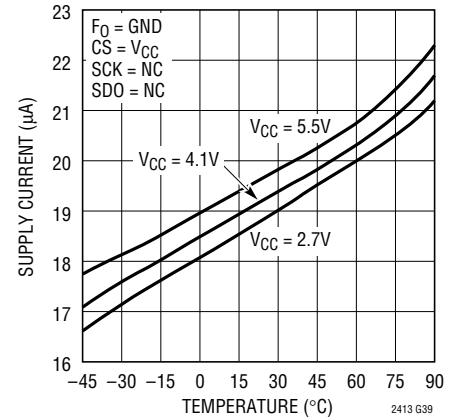
Conversion Current vs Temperature ( $T_A$ )



Conversion Current vs Output Data Rate



Sleep Current vs Temperature ( $T_A$ )



## PIN FUNCTIONS

**GND (Pins 1, 7, 8, 9, 10, 15, 16):** Ground. Multiple ground pins internally connected for optimum ground current flow and  $V_{CC}$  decoupling. Connect each one of these pins to a ground plane through a low impedance connection. All seven pins must be connected to ground for proper operation.

**$V_{CC}$  (Pin 2):** Positive Supply Voltage. Bypass to GND (Pin 1) with a  $10\mu\text{F}$  tantalum capacitor in parallel with  $0.1\mu\text{F}$  ceramic capacitor as close to the part as possible.

**$\text{REF}^+$  (Pin 3),  $\text{REF}^-$  (Pin 4):** Differential Reference Input. The voltage on these pins can have any value between GND and  $V_{CC}$  as long as the reference positive input,  $\text{REF}^+$ , is maintained more positive than the reference negative input,  $\text{REF}^-$ , by at least  $0.1\text{V}$ .

**$\text{IN}^+$  (Pin 5),  $\text{IN}^-$  (Pin 6):** Differential Analog Input. The voltage on these pins can have any value between  $\text{GND} - 0.3\text{V}$  and  $V_{CC} + 0.3\text{V}$ . Within these limits, the converter bipolar input range ( $V_{\text{IN}} = \text{IN}^+ - \text{IN}^-$ ) extends from  $-0.5 \cdot (V_{\text{REF}})$  to  $0.5 \cdot (V_{\text{REF}})$ . Outside this input range, the converter produces unique overrange and underrange output codes.

**$\overline{\text{CS}}$  (Pin 11):** Active LOW Digital Input. A LOW on this pin enables the SDO digital output and wakes up the ADC. Following each conversion, the ADC automatically enters the Sleep mode and remains in this low power state as long as  $\overline{\text{CS}}$  is HIGH. A LOW-to-HIGH transition on  $\overline{\text{CS}}$  during the Data Output transfer aborts the data transfer and starts a new conversion.

**SDO (Pin 12):** Three-State Digital Output. During the Data Output period, this pin is used as serial data output. When the chip select  $\overline{\text{CS}}$  is HIGH ( $\overline{\text{CS}} = V_{CC}$ ), the SDO pin is in a high impedance state. During the Conversion and Sleep periods, this pin is used as the conversion status output. The conversion status can be observed by pulling  $\overline{\text{CS}}$  LOW.

**SCK (Pin 13):** Bidirectional Digital Clock Pin. In Internal Serial Clock Operation mode, SCK is used as digital output for the internal serial interface clock during the Data Output period. In External Serial Clock Operation mode, SCK is used as digital input for the external serial interface clock during the Data Output period. A weak internal pull-up is automatically activated in Internal Serial Clock Operation mode. The Serial Clock Operation mode is determined by the logic level applied to the SCK pin at power up or during the most recent falling edge of  $\overline{\text{CS}}$ .

**$F_0$  (Pin 14):** Frequency Control Pin. Digital input that controls the ADC's notch frequencies and conversion time. When the  $F_0$  pin is connected to GND ( $F_0 = 0\text{V}$ ), the converter uses its internal oscillator and the digital filter rejects 50Hz and 60Hz simultaneously. When the  $F_0$  pin is driven by an external clock signal with a frequency  $f_{\text{EOSC}}$ , the converter uses this signal as its system clock and the digital filter has 87dB minimum rejection in the range  $f_{\text{EOSC}}/2560 \pm 14\%$  and 110dB minimum rejection at  $f_{\text{EOSC}}/2560 \pm 4\%$ .

## FUNCTIONAL BLOCK DIAGRAM

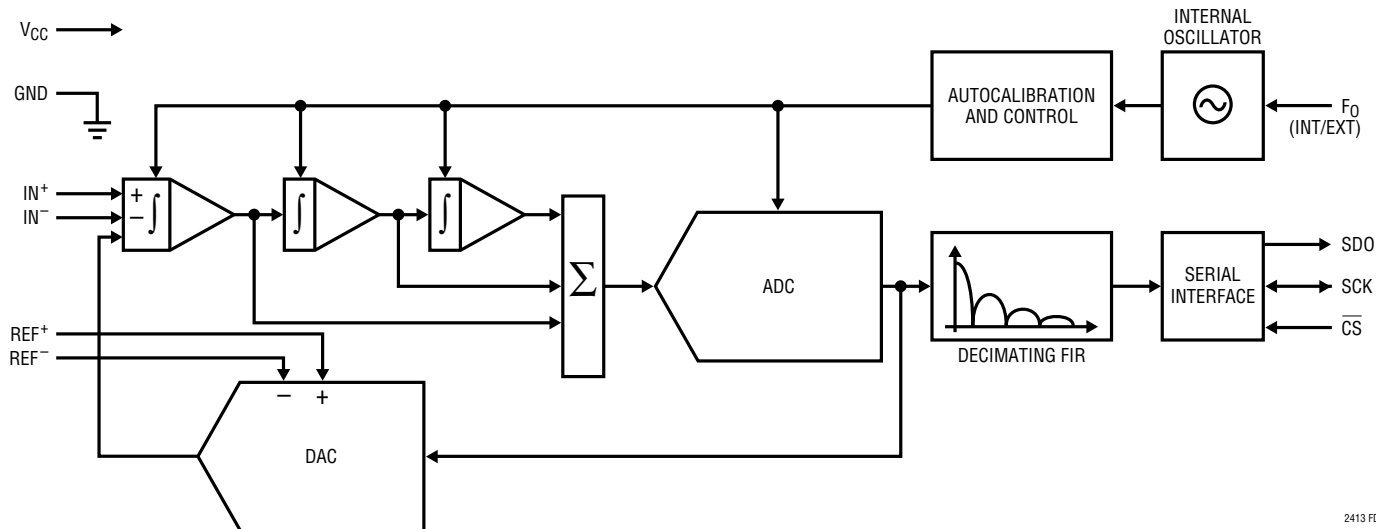


Figure 1. Functional Block Diagram

## TEST CIRCUITS



## APPLICATIONS INFORMATION

### CONVERTER OPERATION

#### Converter Operation Cycle

The LTC2413 is a low power, delta-sigma analog-to-digital converter with an easy to use 3-wire serial interface. Its operation is made up of three states. The converter operating cycle begins with the conversion, followed by the low power sleep state and ends with the data output (see Figure 2). The 3-wire interface consists of serial data output (SDO), serial clock (SCK) and chip select ( $\overline{CS}$ ).

Initially, the LTC2413 performs a conversion. Once the conversion is complete, the device enters the sleep state. While in this sleep state, power consumption is reduced by an order of magnitude. The part remains in the sleep state as long as  $\overline{CS}$  is HIGH. The conversion result is held indefinitely in a static shift register while the converter is in the sleep state.

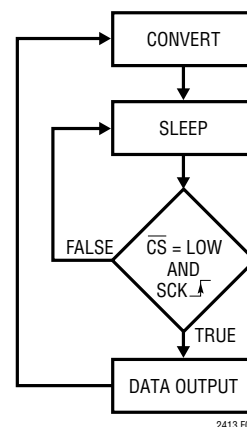


Figure 2. LTC2413 State Transition Diagram

## APPLICATIONS INFORMATION

Once  $\overline{CS}$  is pulled LOW, the device begins outputting the conversion result. There is no latency in the conversion result. The data output corresponds to the conversion just performed. This result is shifted out on the serial data out pin (SDO) under the control of the serial clock (SCK). Data is updated on the falling edge of SCK allowing the user to reliably latch data on the rising edge of SCK (see Figure 3). The data output state is concluded once 32 bits are read out of the ADC or when  $\overline{CS}$  is brought HIGH. The device automatically initiates a new conversion and the cycle repeats.

Through timing control of the  $\overline{CS}$  and SCK pins, the LTC2413 offers several flexible modes of operation (internal or external SCK and free-running conversion modes). These various modes do not require programming configuration registers; moreover, they do not disturb the cyclic operation described above. These modes of operation are described in detail in the Serial Interface Timing Modes section.

### Conversion Clock

A major advantage the delta-sigma converter offers over conventional type converters is an on-chip digital filter (commonly implemented as a sinc or comb filter). For high resolution, low frequency applications, this filter is designed to simultaneously reject line frequencies of 50Hz and 60Hz plus their harmonics. The filter rejection performance is directly related to the accuracy of the converter system clock. The LTC2413 incorporates a highly accurate on-chip oscillator. This eliminates the need for external frequency setting components such as crystals or oscillators. The LTC2413 achieves a minimum of 87dB over the range of 49Hz to 61.2Hz.

### Ease of Use

The LTC2413 data output has no latency, filter settling delay or redundant data associated with the conversion cycle. There is a one-to-one correspondence between the conversion and the output data. Therefore, multiplexing multiple analog voltages is easy.

The LTC2413 performs offset and full-scale calibrations in every conversion cycle. This calibration is transparent to the user and has no effect on the cyclic operation described above. The advantage of continuous calibration is extreme stability of offset and full-scale readings with respect to time, supply voltage change and temperature drift.

### Power-Up Sequence

The LTC2413 automatically enters an internal reset state when the power supply voltage  $V_{CC}$  drops below approximately 2.2V. This feature guarantees the integrity of the conversion result and of the serial interface mode selection. (See the 2-wire I/O sections in the Serial Interface Timing Modes section.)

When the  $V_{CC}$  voltage rises above this critical threshold, the converter creates an internal power-on-reset (POR) signal with a duration of approximately 0.5ms. The POR signal clears all internal registers. Following the POR signal, the LTC2413 starts a normal conversion cycle and follows the succession of states described above. The first conversion result following POR is accurate within the specifications of the device if the power supply voltage is restored within the operating range (2.7V to 5.5V) before the end of the POR time interval.

### Reference Voltage Range

This converter accepts a truly differential external reference voltage. The absolute/common mode voltage specification for the  $REF^+$  and  $REF^-$  pins covers the entire range from GND to  $V_{CC}$ . For correct converter operation, the  $REF^+$  pin must always be more positive than the  $REF^-$  pin.

The LTC2413 can accept a differential reference voltage from 0.1V to  $V_{CC}$ . The converter output noise is determined by the thermal noise of the front-end circuits, and as such, its value in nanovolts is nearly constant with reference voltage. A decrease in reference voltage will not significantly improve the converter's effective resolution. On the other hand, a reduced reference voltage will improve the converter's overall INL performance. A reduced reference voltage will also improve the converter performance when operated with an external conversion clock (external  $F_0$  signal) at substantially higher output data rates (see the Output Data Rate section).

## APPLICATIONS INFORMATION

### Input Voltage Range

The analog input is truly differential with an absolute/common mode range for the  $IN^+$  and  $IN^-$  input pins extending from  $GND - 0.3V$  to  $V_{CC} + 0.3V$ . Outside these limits, the ESD protection devices begin to turn on and the errors due to input leakage current increase rapidly. Within these limits, the LTC2413 converts the bipolar differential input signal,  $V_{IN} = IN^+ - IN^-$ , from  $-FS = -0.5 \cdot V_{REF}$  to  $+FS = 0.5 \cdot V_{REF}$  where  $V_{REF} = REF^+ - REF^-$ . Outside this range, the converter indicates the overrange or the underrange condition using distinct output codes.

Input signals applied to  $IN^+$  and  $IN^-$  pins may extend by 300mV below ground and above  $V_{CC}$ . In order to limit any fault current, resistors of up to 5k may be added in series with the  $IN^+$  and  $IN^-$  pins without affecting the performance of the device. In the physical layout, it is important to maintain the parasitic capacitance of the connection between these series resistors and the corresponding pins as low as possible; therefore, the resistors should be located as close as practical to the pins. The effect of the series resistance on the converter accuracy can be evaluated from the curves presented in the Input Current/Reference Current sections. In addition, series resistors will introduce a temperature dependent offset error due to the input leakage current. A 1nA input leakage current will develop a 1ppm offset error on a 5k resistor if  $V_{REF} = 5V$ . This error has a very strong temperature dependency.

### Output Data Format

The LTC2413 serial output data stream is 32 bits long. The first 3 bits represent status information indicating the sign and conversion state. The next 24 bits are the conversion result, MSB first. The remaining 5 bits are sub LSBs beyond the 24-bit level that may be included in averaging or discarded without loss of resolution. The third and fourth bits together are also used to indicate an underrange condition (the differential input voltage is below  $-FS$ ) or an overrange condition (the differential input voltage is above  $+FS$ ).

Bit 31 (first output bit) is the end of conversion ( $\overline{EOC}$ ) indicator. This bit is available at the SDO pin during the conversion and sleep states whenever the  $\overline{CS}$  pin is LOW.

This bit is HIGH during the conversion and goes LOW when the conversion is complete.

Bit 30 (second output bit) is a dummy bit (DMY) and is always LOW.

Bit 29 (third output bit) is the conversion result sign indicator (SIG). If  $V_{IN}$  is  $>0$ , this bit is HIGH. If  $V_{IN}$  is  $<0$ , this bit is LOW.

Bit 28 (fourth output bit) is the most significant bit (MSB) of the result. This bit in conjunction with Bit 29 also provides the underrange or overrange indication. If both Bit 29 and Bit 28 are HIGH, the differential input voltage is above  $+FS$ . If both Bit 29 and Bit 28 are LOW, the differential input voltage is below  $-FS$ .

The function of these bits is summarized in Table 1.

**Table 1. LTC2413 Status Bits**

Input Range	Bit 31 $\overline{EOC}$	Bit 30 DMY	Bit 29 SIG	Bit 28 MSB
$V_{IN} \geq 0.5 \cdot V_{REF}$	0	0	1	1
$0V \leq V_{IN} < 0.5 \cdot V_{REF}$	0	0	1	0
$-0.5 \cdot V_{REF} \leq V_{IN} < 0V$	0	0	0	1
$V_{IN} < -0.5 \cdot V_{REF}$	0	0	0	0

Bits 28-5 are the 24-bit conversion result MSB first.

Bit 5 is the least significant bit (LSB).

Bits 4-0 are sub LSBs below the 24-bit level. Bits 4-0 may be included in averaging or discarded without loss of resolution.

Data is shifted out of the SDO pin under control of the serial clock (SCK), see Figure 3. Whenever  $\overline{CS}$  is HIGH, SDO remains high impedance and any externally generated SCK clock pulses are ignored by the internal data out shift register.

In order to shift the conversion result out of the device,  $\overline{CS}$  must first be driven LOW.  $\overline{EOC}$  is seen at the SDO pin of the device once  $\overline{CS}$  is pulled LOW.  $\overline{EOC}$  changes real time from HIGH to LOW at the completion of a conversion. This signal may be used as an interrupt for an external microcontroller. Bit 31 ( $\overline{EOC}$ ) can be captured on the first rising edge of SCK. Bit 30 is shifted out of the device on the first falling edge of SCK. The final data bit (Bit 0) is shifted out on the falling edge of the 31st SCK and may be latched

## APPLICATIONS INFORMATION

on the rising edge of the 32nd SCK pulse. On the falling edge of the 32nd SCK pulse, SDO goes HIGH indicating the initiation of a new conversion cycle. This bit serves as EOC (Bit 31) for the next conversion cycle. Table 2 summarizes the output data format.

As long as the voltage on the IN<sup>+</sup> and IN<sup>-</sup> pins is maintained within the  $-0.3V$  to  $(V_{CC} + 0.3V)$  absolute maximum operating range, a conversion result is generated for any differential input voltage  $V_{IN}$  from  $-FS = -0.5 \cdot V_{REF}$  to  $+FS = 0.5 \cdot V_{REF}$ . For differential input voltages greater than  $+FS$ , the conversion result is clamped to the value corresponding to the  $+FS + 1LSB$ . For differential input voltages below  $-FS$ , the conversion result is clamped to the value corresponding to  $-FS - 1LSB$ .

### Simultaneous Frequency Rejection

The LTC2413 internal oscillator provides better than 87dB normal mode rejection over the range of 49Hz to 61.2Hz as shown in Figure 4. For this simultaneous 50Hz/60Hz rejection,  $F_0$  should be connected to GND.

When a fundamental rejection frequency different from the range 49Hz to 61.2Hz is required or when the converter must be synchronized with an outside source, the LTC2413 can operate with an external conversion clock. The converter automatically detects the presence of an external clock signal at the  $F_0$  pin and turns off the internal oscillator. The frequency  $f_{EOSC}$  of the external signal must be at least 2560Hz to be detected. The external clock signal duty cycle is not significant as long as the minimum and maximum specifications for the high and low periods,  $t_{HEO}$  and  $t_{LEO}$ , are observed.

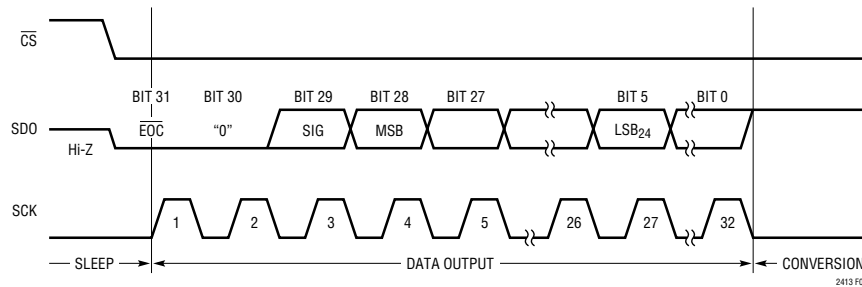


Figure 3. Output Data Timing

Table 2. LTC2413 Output Data Format

Differential Input Voltage $V_{IN}^*$	Bit 31 EOC	Bit 30 DMY	Bit 29 SIG	Bit 28 MSB	Bit 27	Bit 26	Bit 25	...	Bit 0
$V_{IN}^* \geq 0.5 \cdot V_{REF}^{**}$	0	0	1	1	0	0	0	...	0
$0.5 \cdot V_{REF}^{**} - 1LSB$	0	0	1	0	1	1	1	...	1
$0.25 \cdot V_{REF}^{**}$	0	0	1	0	1	0	0	...	0
$0.25 \cdot V_{REF}^{**} - 1LSB$	0	0	1	0	0	1	1	...	1
0	0	0	1	0	0	0	0	...	0
-1LSB	0	0	0	1	1	1	1	...	1
$-0.25 \cdot V_{REF}^{**}$	0	0	0	1	1	0	0	...	0
$-0.25 \cdot V_{REF}^{**} - 1LSB$	0	0	0	1	0	1	1	...	1
$-0.5 \cdot V_{REF}^{**}$	0	0	0	1	0	0	0	...	0
$V_{IN}^* < -0.5 \cdot V_{REF}^{**}$	0	0	0	0	1	1	1	...	1

\*The differential input voltage  $V_{IN} = IN^+ - IN^-$ .

\*\*The differential reference voltage  $V_{REF} = REF^+ - REF^-$ .

## APPLICATIONS INFORMATION

While operating with an external conversion clock of a frequency  $f_{EOSC}$ , the LTC2413 provides better than 110dB normal mode rejection in a frequency range  $f_{EOSC}/2560 \pm 4\%$ . The normal mode rejection as a function of the input frequency deviation from  $f_{EOSC}/2560$  is shown in Figure 5.

Whenever an external clock is not present at the  $F_0$  pin the converter automatically activates its internal oscillator and enters the Internal Conversion Clock mode. The LTC2413 operation will not be disturbed if the change of conversion clock source occurs during the sleep state or during the data output state while the converter uses an external serial clock. If the change occurs during the conversion state, the result of the conversion in progress may be outside specifications but the following conversions will not be affected. If the change occurs during the data output state and the converter is in the Internal SCK mode, the serial clock duty cycle may be affected but the serial data stream will remain valid.

Table 3 summarizes the duration of each state and the achievable output data rate as a function of  $F_0$ .

### SERIAL INTERFACE PINS

The LTC2413 transmits the conversion results and receives the start of conversion command through a synchronous 3-wire interface. During the conversion and sleep states, this interface can be used to assess the converter status and during the data output state it is used to read the conversion result.

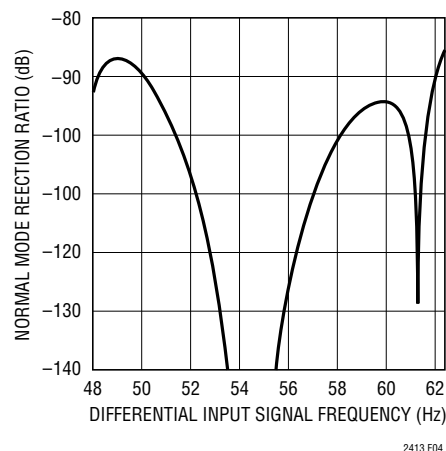


Figure 4. LTC2413 Normal Mode Rejection When Using an Internal Oscillator

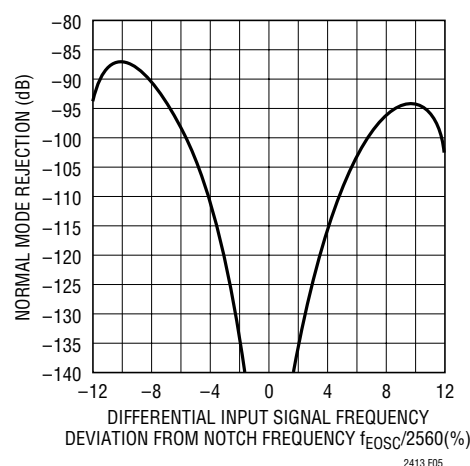


Figure 5. LTC2413 Normal Mode Rejection When Using an External Oscillator of Frequency  $f_{EOSC}$

Table 3. LTC2413 State Duration

State	Operating Mode		Duration
CONVERT	Internal Oscillator	$F_0 = \text{LOW}$ Simultaneous 50Hz/60Hz Rejection	147ms, Output Data Rate $\leq 6.8$ Readings/s
	External Oscillator	$F_0 = \text{External Oscillator}$ with Frequency $f_{EOSC}$ kHz ( $f_{EOSC}/2560$ Rejection)	$20510/f_{EOSC}$ s, Output Data Rate $\leq f_{EOSC}/20510$ Readings/s
SLEEP			As Long As $\overline{CS} = \text{HIGH}$ Until $\overline{CS} = \text{LOW}$ and $\text{SCK} \downarrow$
DATA OUTPUT	Internal Serial Clock	$F_0 = \text{LOW}$ (Internal Oscillator)	As Long As $\overline{CS} = \text{LOW}$ But Not Longer Than 1.83ms (32 SCK cycles)
		$F_0 = \text{External Oscillator}$ with Frequency $f_{EOSC}$ kHz	As Long As $\overline{CS} = \text{LOW}$ But Not Longer Than $256/f_{EOSC}$ ms (32 SCK cycles)
	External Serial Clock with Frequency $f_{SCK}$ kHz		As Long As $\overline{CS} = \text{LOW}$ But Not Longer Than $32/f_{SCK}$ ms (32 SCK cycles)

sn2413 2413fs

## APPLICATIONS INFORMATION

### Serial Clock Input/Output (SCK)

The serial clock signal present on SCK (Pin 13) is used to synchronize the data transfer. Each bit of data is shifted out the SDO pin on the falling edge of the serial clock.

In the Internal SCK mode of operation, the SCK pin is an output and the LTC2413 creates its own serial clock by dividing the internal conversion clock by 8. In the External SCK mode of operation, the SCK pin is used as input. The internal or external SCK mode is selected on power-up and then reselected every time a HIGH-to-LOW transition is detected at the CS pin. If SCK is HIGH or floating at power-up or during this transition, the converter enters the internal SCK mode. If SCK is LOW at power-up or during this transition, the converter enters the external SCK mode.

### Serial Data Output (SDO)

The serial data output pin, SDO (Pin 12), provides the result of the last conversion as a serial bit stream (MSB first) during the data output state. In addition, the SDO pin is used as an end of conversion indicator during the conversion and sleep states.

When  $\overline{CS}$  (Pin 11) is HIGH, the SDO driver is switched to a high impedance state. This allows sharing the serial interface with other devices. If  $\overline{CS}$  is LOW during the convert or sleep state, SDO will output  $\overline{EOC}$ . If  $\overline{CS}$  is LOW during the conversion phase, the  $\overline{EOC}$  bit appears HIGH on the SDO pin. Once the conversion is complete,  $\overline{EOC}$  goes LOW. The device remains in the sleep state until the first rising edge of SCK occurs while  $\overline{CS} = \text{LOW}$ .

### Chip Select Input ( $\overline{CS}$ )

The active LOW chip select,  $\overline{CS}$  (Pin 11), is used to test the conversion status and to enable the data output transfer as described in the previous sections.

In addition, the  $\overline{CS}$  signal can be used to trigger a new conversion cycle before the entire serial data transfer has been completed. The LTC2413 will abort any serial data transfer in progress and start a new conversion cycle anytime a LOW-to-HIGH transition is detected at the  $\overline{CS}$  pin after the converter has entered the data output state (i.e., after the first rising edge of SCK occurs with  $\overline{CS} = \text{LOW}$ ).

Finally,  $\overline{CS}$  can be used to control the free-running modes of operation, see Serial Interface Timing Modes section. Grounding  $\overline{CS}$  will force the ADC to continuously convert at the maximum output rate selected by  $F_0$ . Tying a capacitor to  $\overline{CS}$  will reduce the output rate and power dissipation by a factor proportional to the capacitor's value, see Figures 13 to 15.

## SERIAL INTERFACE TIMING MODES

The LTC2413's 3-wire interface is SPI and MICROWIRE compatible. This interface offers several flexible modes of operation. These include internal/external serial clock, 2- or 3-wire I/O, single cycle conversion and autostart. The following sections describe each of these serial interface timing modes in detail. In all these cases, the converter can use the internal oscillator ( $F_0 = \text{LOW}$ ) or an external oscillator connected to the  $F_0$  pin. Refer to Table 4 for a summary.

### External Serial Clock, Single Cycle Operation (SPI/MICROWIRE Compatible)

This timing mode uses an external serial clock to shift out the conversion result and a  $\overline{CS}$  signal to monitor and control the state of the conversion cycle, see Figure 6.

Table 4. LTC2413 Interface Timing Modes

Configuration	SCK Source	Conversion Cycle Control	Data Output Control	Connection and Waveforms
External SCK, Single Cycle Conversion	External	$\overline{CS}$ and SCK	$\overline{CS}$ and SCK	Figures 6, 7
External SCK, 2-Wire I/O	External	SCK	SCK	Figure 8
Internal SCK, Single Cycle Conversion	Internal	$\overline{CS} \downarrow$	$\overline{CS} \downarrow$	Figures 9, 10
Internal SCK, 2-Wire I/O, Continuous Conversion	Internal	Continuous	Internal	Figure 11
Internal SCK, Autostart Conversion	Internal	$C_{EXT}$	Internal	Figure 12

sn2413 2413fs



## APPLICATIONS INFORMATION

The serial clock mode is selected on the falling edge of  $\overline{CS}$ . To select the external serial clock mode, the serial clock pin (SCK) must be LOW during each  $\overline{CS}$  falling edge.

The serial data output pin (SDO) is Hi-Z as long as  $\overline{CS}$  is HIGH. At any time during the conversion cycle,  $\overline{CS}$  may be pulled LOW in order to monitor the state of the converter. While  $\overline{CS}$  is pulled LOW,  $\overline{EOC}$  is output to the SDO pin.  $\overline{EOC} = 1$  while a conversion is in progress and  $\overline{EOC} = 0$  if the device is in the sleep state. Independent of  $\overline{CS}$ , the device automatically enters the low power sleep state once the conversion is complete.

When the device is in the sleep state ( $\overline{EOC} = 0$ ), its conversion result is held in an internal static shift register. The device remains in the sleep state until the first rising edge of SCK is seen while  $\overline{CS}$  is LOW. Data is shifted out the SDO pin on each falling edge of SCK. This enables external circuitry to latch the output on the rising edge of SCK.  $\overline{EOC}$  can be latched on the first rising edge of SCK and the last bit of the conversion result can be latched on the 32nd rising edge of SCK. On the 32nd falling edge of SCK, the device begins a new conversion. SDO goes HIGH ( $\overline{EOC} = 1$ ) indicating a conversion is in progress.

At the conclusion of the data cycle,  $\overline{CS}$  may remain LOW and  $\overline{EOC}$  monitored as an end-of-conversion interrupt. Alternatively,  $\overline{CS}$  may be driven HIGH setting SDO to Hi-Z.

As described above,  $\overline{CS}$  may be pulled LOW at any time in order to monitor the conversion status.

Typically,  $\overline{CS}$  remains LOW during the data output state. However, the data output state may be aborted by pulling  $\overline{CS}$  HIGH anytime between the first rising edge and the 32nd falling edge of SCK, see Figure 7. On the rising edge of  $\overline{CS}$ , the device aborts the data output state and immediately initiates a new conversion. This is useful for systems not requiring all 32 bits of output data, aborting an invalid conversion cycle or synchronizing the start of a conversion.

### External Serial Clock, 2-Wire I/O

This timing mode utilizes a 2-wire serial I/O interface. The conversion result is shifted out of the device by an externally generated serial clock (SCK) signal, see Figure 8.  $\overline{CS}$  may be permanently tied to ground, simplifying the user interface or isolation barrier.

The external serial clock mode is selected at the end of the power-on reset (POR) cycle. The POR cycle is concluded approximately 0.5ms after  $V_{CC}$  exceeds 2.2V. The level applied to SCK at this time determines if SCK is internal or external. SCK must be driven LOW prior to the end of POR in order to enter the external serial clock timing mode.

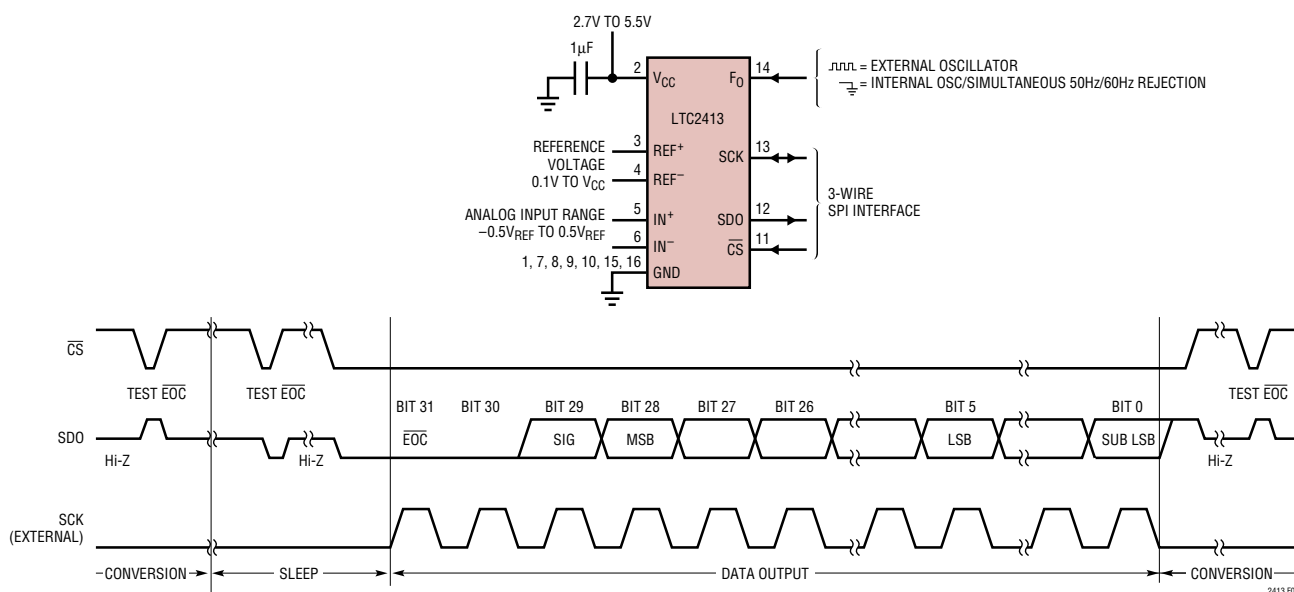


Figure 6. External Serial Clock, Single Cycle Operation

APPLICATIONS INFORMATION

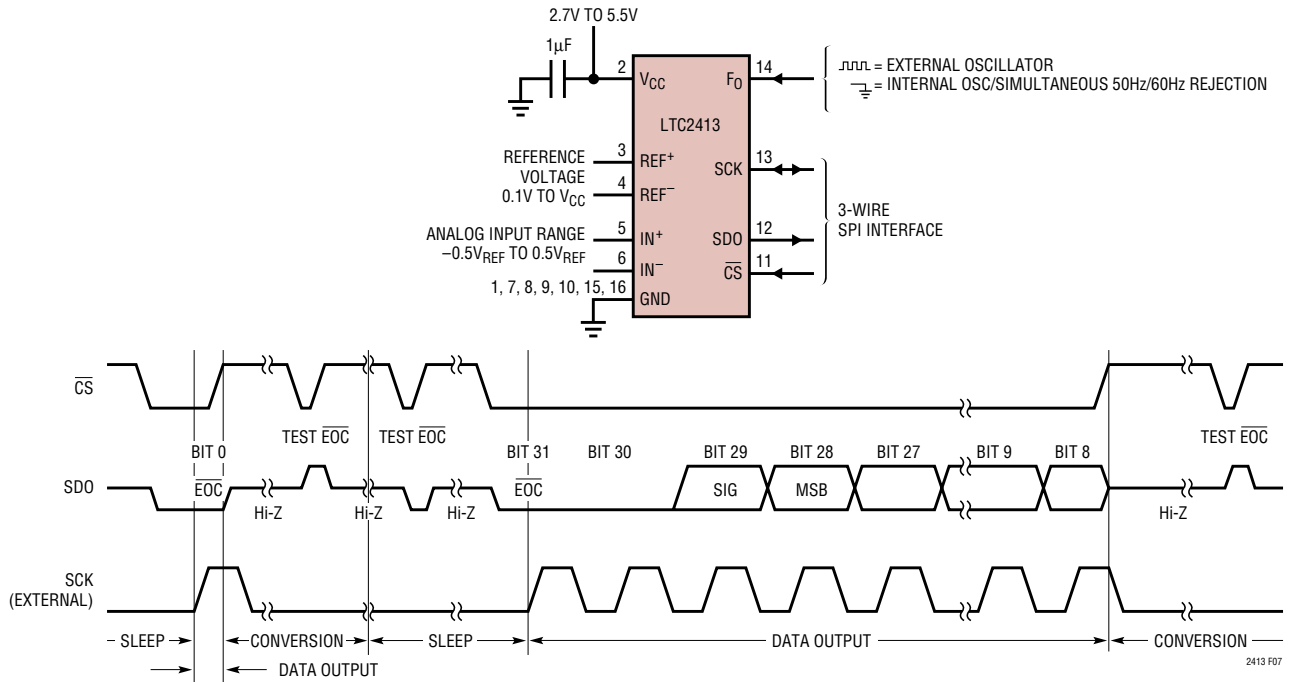


Figure 7. External Serial Clock, Reduced Data Output Length

Since  $\overline{CS}$  is tied LOW, the end-of-conversion ( $\overline{EOC}$ ) can be continuously monitored at the SDO pin during the convert and sleep states.  $\overline{EOC}$  may be used as an interrupt to an external controller indicating the conversion result is ready.  $\overline{EOC} = 1$  while the conversion is in progress and  $\overline{EOC} = 0$  once the conversion enters the low power sleep state. On the falling edge of  $\overline{EOC}$ , the conversion result is loaded into an internal static shift register. The device remains in the sleep state until the first rising edge of SCK. Data is shifted out the SDO pin on each falling edge of SCK enabling external circuitry to latch data on the rising edge of SCK.  $\overline{EOC}$  can be latched on the first rising edge of SCK. On the 32nd falling edge of SCK, SDO goes HIGH ( $\overline{EOC} = 1$ ) indicating a new conversion has begun.

Internal Serial Clock, Single Cycle Operation

This timing mode uses an internal serial clock to shift out the conversion result and a  $\overline{CS}$  signal to monitor and control the state of the conversion cycle, see Figure 9.

In order to select the internal serial clock timing mode, the serial clock pin (SCK) must be floating (Hi-Z) or pulled HIGH prior to the falling edge of  $\overline{CS}$ . The device will not

enter the internal serial clock mode if SCK is driven LOW on the falling edge of  $\overline{CS}$ . An internal weak pull-up resistor is active on the SCK pin during the falling edge of  $\overline{CS}$ ; therefore, the internal serial clock timing mode is automatically selected if SCK is not externally driven.

The serial data output pin (SDO) is Hi-Z as long as  $\overline{CS}$  is HIGH. At any time during the conversion cycle,  $\overline{CS}$  may be pulled LOW in order to monitor the state of the converter. Once  $\overline{CS}$  is pulled LOW, SCK goes LOW and  $\overline{EOC}$  is output to the SDO pin.  $\overline{EOC} = 1$  while a conversion is in progress and  $\overline{EOC} = 0$  if the device is in the sleep state.

When testing  $\overline{EOC}$ , if the conversion is complete ( $\overline{EOC} = 0$ ), the device will exit the sleep state and enter the data output state if  $\overline{CS}$  remains LOW. In order to prevent the device from exiting the low power sleep state,  $\overline{CS}$  must be pulled HIGH before the first rising edge of SCK. In the internal SCK timing mode, SCK goes HIGH and the device begins outputting data at time  $t_{EOCtest}$  after the falling edge of  $\overline{CS}$  (if  $\overline{EOC} = 0$ ) or  $t_{EOCtest}$  after  $\overline{EOC}$  goes LOW (if  $\overline{CS}$  is LOW during the falling edge of  $\overline{EOC}$ ). The value of  $t_{EOCtest}$  is 26µs if the device is using its internal oscillator ( $F_0 = \text{logic LOW}$ ). If  $F_0$  is driven by an external oscillator of frequency  $f_{osc}$ ,

sn2413 2413is

# APPLICATIONS INFORMATION

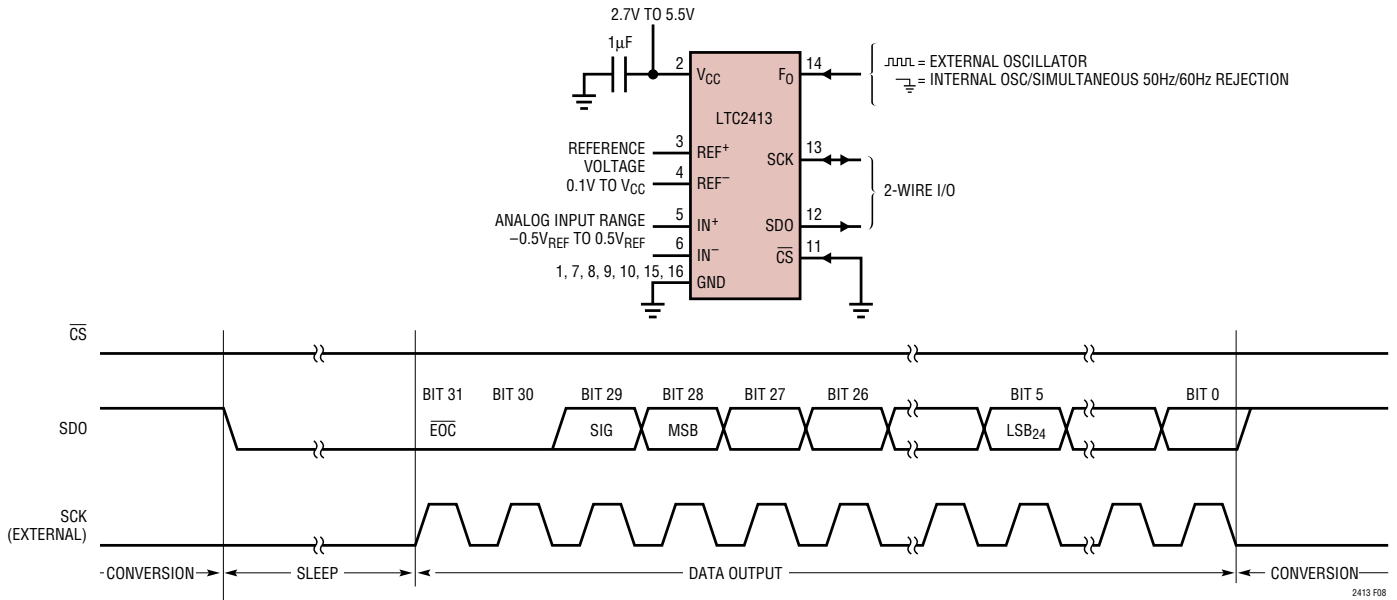


Figure 8. External Serial Clock,  $\overline{CS} = 0$  Operation

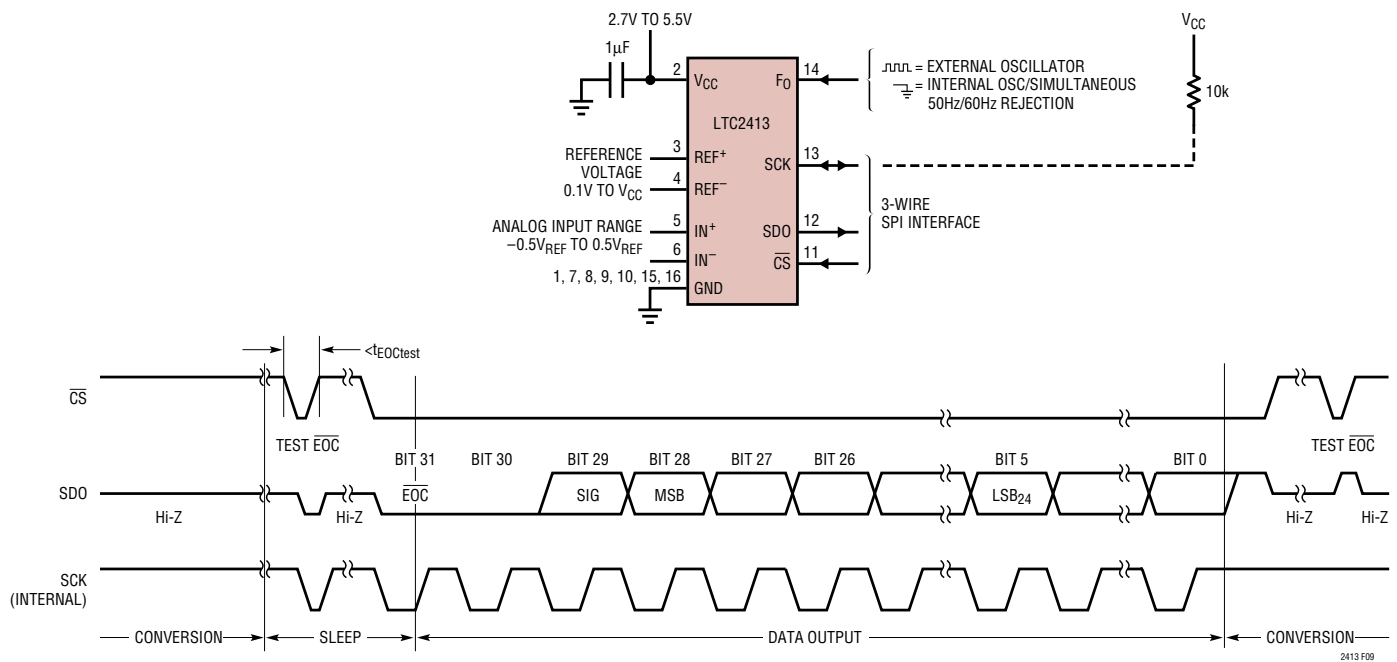


Figure 9. Internal Serial Clock, Single Cycle Operation

## APPLICATIONS INFORMATION

then  $t_{EOCtest}$  is  $3.6/f_{OSC}$ . If  $\overline{CS}$  is pulled HIGH before time  $t_{EOCtest}$ , the device remains in the sleep state. The conversion result is held in the internal static shift register.

If  $\overline{CS}$  remains LOW longer than  $t_{EOCtest}$ , the first rising edge of SCK will occur and the conversion result is serially shifted out of the SDO pin. The data output cycle begins on this first rising edge of SCK and concludes after the 32nd rising edge. Data is shifted out the SDO pin on each falling edge of SCK. The internally generated serial clock is output to the SCK pin. This signal may be used to shift the conversion result into external circuitry.  $\overline{EOC}$  can be latched on the first rising edge of SCK and the last bit of the conversion result on the 32nd rising edge of SCK. After the 32nd rising edge, SDO goes HIGH ( $\overline{EOC} = 1$ ), SCK stays HIGH and a new conversion starts.

Typically,  $\overline{CS}$  remains LOW during the data output state. However, the data output state may be aborted by pulling  $\overline{CS}$  HIGH anytime between the first and 32nd rising edge of SCK, see Figure 10. On the rising edge of  $\overline{CS}$ , the device aborts the data output state and immediately initiates a

new conversion. This is useful for systems not requiring all 32 bits of output data, aborting an invalid conversion cycle, or synchronizing the start of a conversion. If  $\overline{CS}$  is pulled HIGH while the converter is driving SCK LOW, the internal pull-up is not available to restore SCK to a logic HIGH state. This will cause the device to exit the internal serial clock mode on the next falling edge of  $\overline{CS}$ . This can be avoided by adding an external 10k pull-up resistor to the SCK pin or by never pulling  $\overline{CS}$  HIGH when SCK is LOW.

Whenever SCK is LOW, the LTC2413's internal pull-up at pin SCK is disabled. Normally, SCK is not externally driven if the device is in the internal SCK timing mode. However, certain applications may require an external driver on SCK. If this driver goes Hi-Z after outputting a LOW signal, the LTC2413's internal pull-up remains disabled. Hence, SCK remains LOW. On the next falling edge of  $\overline{CS}$ , the device is switched to the external SCK timing mode. By adding an external 10k pull-up resistor to SCK, this pin goes HIGH once the external driver goes Hi-Z. On the next  $\overline{CS}$  falling edge, the device will remain in the internal SCK timing mode.

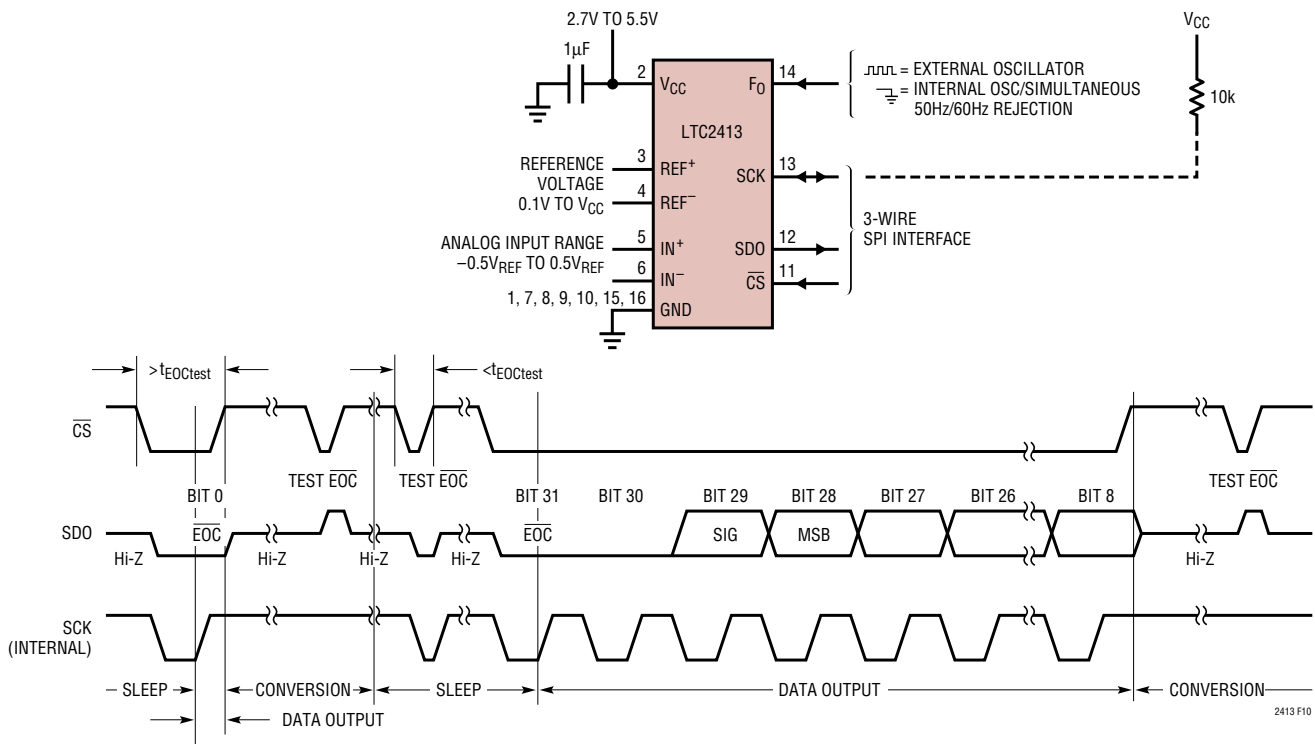


Figure 10. Internal Serial Clock, Reduced Data Output Length

sn2413 2413fs

## APPLICATIONS INFORMATION

A similar situation may occur during the sleep state when  $\overline{CS}$  is pulsed HIGH-LOW-HIGH in order to test the conversion status. If the device is in the sleep state ( $\overline{EOC} = 0$ ), SCK will go LOW. Once  $\overline{CS}$  goes HIGH (within the time period defined above as  $t_{EOCtest}$ ), the internal pull-up is activated. For a heavy capacitive load on the SCK pin, the internal pull-up may not be adequate to return SCK to a HIGH level before  $\overline{CS}$  goes low again. This is not a concern under normal conditions where  $\overline{CS}$  remains LOW after detecting  $\overline{EOC} = 0$ . This situation is easily overcome by adding an external 10k pull-up resistor to the SCK pin.

### Internal Serial Clock, 2-Wire I/O, Continuous Conversion

This timing mode uses a 2-wire, all output (SCK and SDO) interface. The conversion result is shifted out of the device by an internally generated serial clock (SCK) signal, see Figure 11.  $\overline{CS}$  may be permanently tied to ground, simplifying the user interface or isolation barrier.

The internal serial clock mode is selected at the end of the power-on reset (POR) cycle. The POR cycle is concluded approximately 0.5ms after  $V_{CC}$  exceeds 2.2V. An internal

weak pull-up is active during the POR cycle; therefore, the internal serial clock timing mode is automatically selected if SCK is not externally driven LOW (if SCK is loaded such that the internal pull-up cannot pull the pin HIGH, the external SCK mode will be selected).

During the conversion, the SCK and the serial data output pin (SDO) are HIGH ( $\overline{EOC} = 1$ ). Once the conversion is complete, SCK and SDO go LOW ( $\overline{EOC} = 0$ ) indicating the conversion has finished and the device has entered the low power sleep state. The part remains in the sleep state a minimum amount of time (1/2 the internal SCK period) then immediately begins outputting data. The data output cycle begins on the first rising edge of SCK and ends after the 32nd rising edge. Data is shifted out the SDO pin on each falling edge of SCK. The internally generated serial clock is output to the SCK pin. This signal may be used to shift the conversion result into external circuitry.  $\overline{EOC}$  can be latched on the first rising edge of SCK and the last bit of the conversion result can be latched on the 32nd rising edge of SCK. After the 32nd rising edge, SDO goes HIGH ( $\overline{EOC} = 1$ ) indicating a new conversion is in progress. SCK remains HIGH during the conversion.

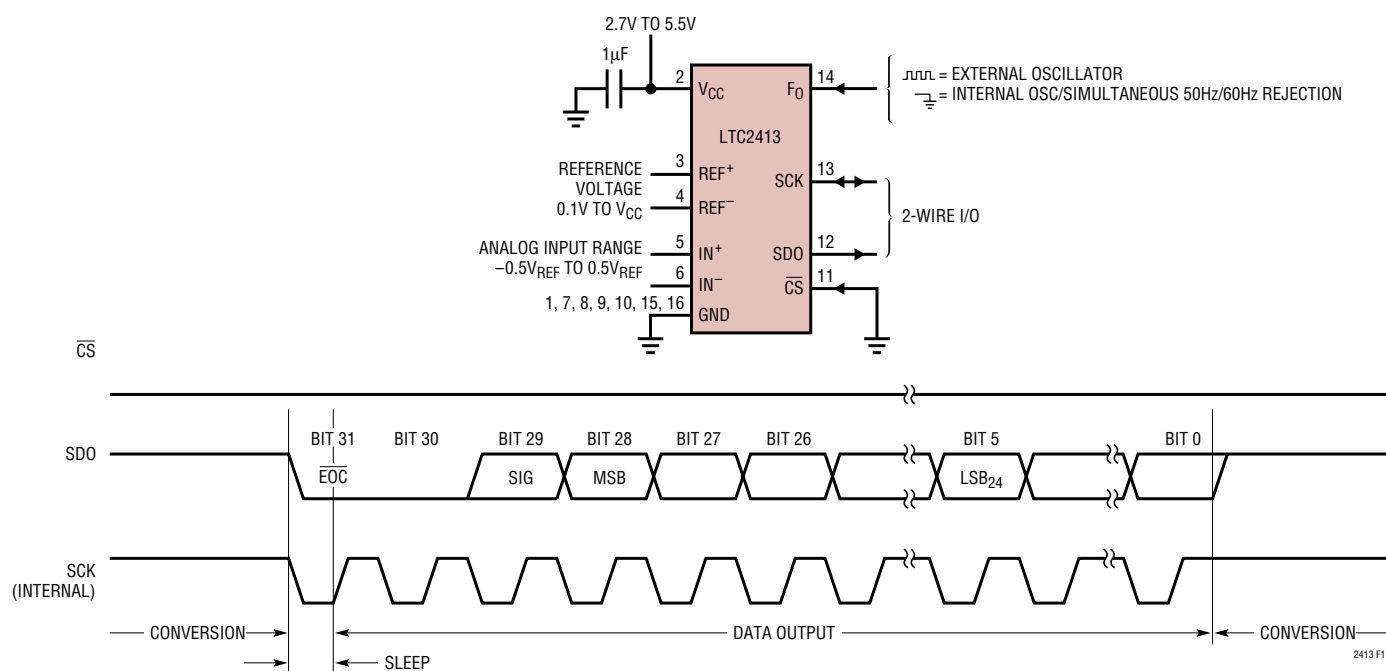


Figure 11. Internal Serial Clock,  $\overline{CS} = 0$  Continuous Operation

## APPLICATIONS INFORMATION

### Internal Serial Clock, Autostart Conversion

This timing mode is identical to the internal serial clock, 2-wire I/O described above with one additional feature. Instead of grounding  $\overline{CS}$ , an external timing capacitor is tied to  $\overline{CS}$ .

While the conversion is in progress, the  $\overline{CS}$  pin is held HIGH by an internal weak pull-up. Once the conversion is complete, the device enters the low power sleep state and an internal 25nA current source begins discharging the capacitor tied to  $\overline{CS}$ , see Figure 12. The time the converter spends in the sleep state is determined by the value of the external timing capacitor, see Figures 13 and 14. Once the voltage at  $\overline{CS}$  falls below an internal threshold ( $\approx 1.4V$ ), the device automatically begins outputting data. The data output cycle begins on the first rising edge of SCK and ends on the 32nd rising edge. Data is shifted out the SDO pin on each falling edge of SCK. The internally generated serial clock is output to the SCK pin. This signal may be

used to shift the conversion result into external circuitry. After the 32nd rising edge,  $\overline{CS}$  is pulled HIGH and a new conversion is immediately started. This is useful in applications requiring periodic monitoring and ultralow power. Figure 15 shows the average supply current as a function of capacitance on  $\overline{CS}$ .

It should be noticed that the external capacitor discharge current is kept very small in order to decrease the converter power dissipation in the sleep state. In the autostart mode, the analog voltage on the  $\overline{CS}$  pin cannot be observed without disturbing the converter operation using a regular oscilloscope probe. When using this configuration, it is important to minimize the external leakage current at the  $\overline{CS}$  pin by using a low leakage external capacitor and properly cleaning the PCB surface.

The internal serial clock mode is selected every time the voltage on the  $\overline{CS}$  pin crosses an internal threshold voltage. An internal weak pull-up at the SCK pin is active while

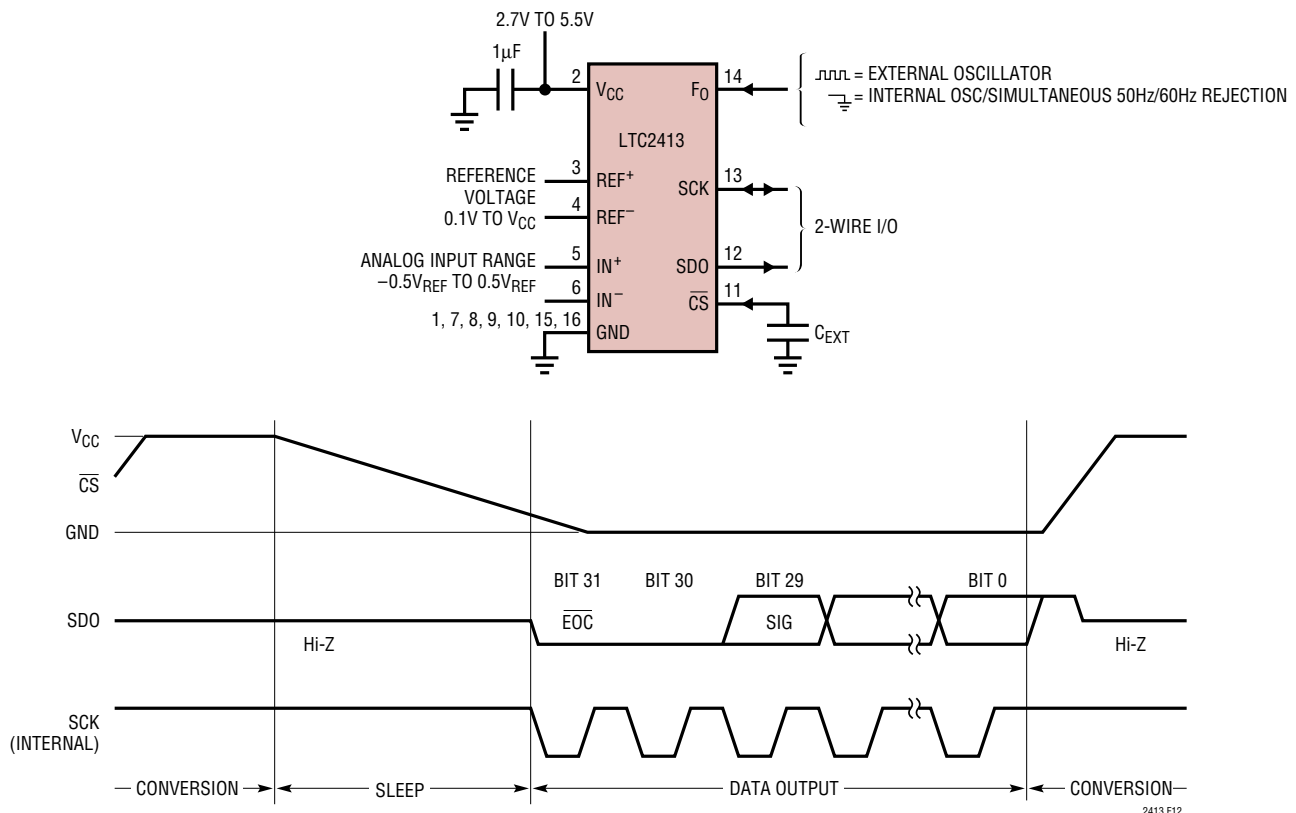


Figure 12. Internal Serial Clock, Autostart Operation

## APPLICATIONS INFORMATION

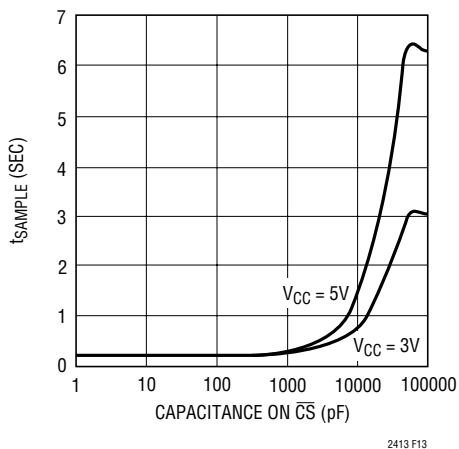


Figure 13.  $\overline{CS}$  Capacitance vs  $t_{SAMPLE}$

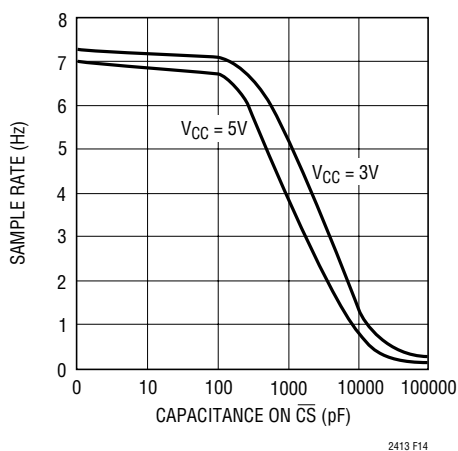


Figure 14.  $\overline{CS}$  Capacitance vs Output Rate

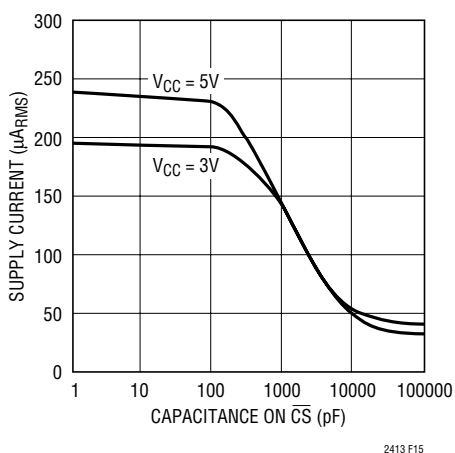


Figure 15.  $\overline{CS}$  Capacitance vs Supply Current

$\overline{CS}$  is discharging; therefore, the internal serial clock timing mode is automatically selected if SCK is floating. It is important to ensure there are no external drivers pulling SCK LOW while  $\overline{CS}$  is discharging.

### PRESERVING THE CONVERTER ACCURACY

The LTC2413 is designed to reduce as much as possible the conversion result sensitivity to device decoupling, PCB layout, antialiasing circuits, line frequency perturbations and so on. Nevertheless, in order to preserve the extreme accuracy capability of this part, some simple precautions are desirable.

### Digital Signal Levels

The LTC2413's digital interface is easy to use. Its digital inputs ( $F_0$ ,  $\overline{CS}$  and SCK in External SCK mode of operation) accept standard TTL/CMOS logic levels and the internal hysteresis receivers can tolerate edge rates as slow as 100 $\mu$ s. However, some considerations are required to take advantage of the exceptional accuracy and low supply current of this converter.

The digital output signals (SDO and SCK in Internal SCK mode of operation) are less of a concern because they are not generally active during the conversion state.

While a digital input signal is in the range 0.5V to ( $V_{CC} - 0.5V$ ), the CMOS input receiver draws additional current from the power supply. It should be noted that, when any one of the digital input signals ( $F_0$ ,  $\overline{CS}$  and SCK in External SCK mode of operation) is within this range, the LTC2413 power supply current may increase even if the signal in question is at a valid logic level. For micropower operation, it is recommended to drive all digital input signals to full CMOS levels [ $V_{IL} < 0.4V$  and  $V_{IH} > (V_{CC} - 0.4V)$ ].

During the conversion period, the undershoot and/or overshoot of a fast digital signal connected to the LTC2413 pins may severely disturb the analog to digital conversion process. Undershoot and overshoot can occur because of the impedance mismatch at the converter pin when the transition time of an external control signal is less than twice the propagation delay from the driver to LTC2413. For reference, on a regular FR-4 board, signal propagation

## APPLICATIONS INFORMATION

velocity is approximately 183ps/inch for internal traces and 170ps/inch for surface traces. Thus, a driver generating a control signal with a minimum transition time of 1ns must be connected to the converter pin through a trace shorter than 2.5 inches. This problem becomes particularly difficult when shared control lines are used and multiple reflections may occur. The solution is to carefully terminate all transmission lines close to their characteristic impedance.

Parallel termination near the LTC2413 pin will eliminate this problem but will increase the driver power dissipation. A series resistor between 27 $\Omega$  and 56 $\Omega$  placed near the driver or near the LTC2413 pin will also eliminate this problem without additional power dissipation. The actual resistor value depends upon the trace impedance and connection topology.

An alternate solution is to reduce the edge rate of the control signals. It should be noted that using very slow edges will increase the converter power supply current during the transition time. The multiple ground pins used in this package configuration, as well as the differential input and reference architecture, reduce substantially the converter's sensitivity to ground currents.

Particular attention must be given to the connection of the  $F_0$  signal when the LTC2413 is used with an external conversion clock. This clock is active during the conversion time and the normal mode rejection provided by the internal digital filter is not very high at this frequency. A normal mode signal of this frequency at the converter reference terminals may result in DC gain and INL errors. A normal mode signal of this frequency at the converter input terminals may result in a DC offset error. Such perturbations may occur due to asymmetric capacitive coupling between the  $F_0$  signal trace and the converter input and/or reference connection traces. An immediate solution is to maintain maximum possible separation between the  $F_0$  signal trace and the input/reference signals. When the  $F_0$  signal is parallel terminated near the converter, substantial AC current is flowing in the loop formed by the  $F_0$  connection trace, the termination and the ground return path. Thus, perturbation signals may be inductively coupled into the converter input and/or refer-

ence. In this situation, the user must reduce to a minimum the loop area for the  $F_0$  signal as well as the loop area for the differential input and reference connections.

### Driving the Input and Reference

The input and reference pins of the LTC2413 converter are directly connected to a network of sampling capacitors. Depending upon the relation between the differential input voltage and the differential reference voltage, these capacitors are switching between these four pins transferring small amounts of charge in the process. A simplified equivalent circuit is shown in Figure 16.

For a simple approximation, the source impedance  $R_S$  driving an analog input pin (IN<sup>+</sup>, IN<sup>-</sup>, REF<sup>+</sup> or REF<sup>-</sup>) can be considered to form, together with  $R_{SW}$  and  $C_{EQ}$  (see Figure 16), a first order passive network with a time constant  $\tau = (R_S + R_{SW}) \cdot C_{EQ}$ . The converter is able to sample the input signal with better than 1ppm accuracy if the sampling period is at least 14 times greater than the input circuit time constant  $\tau$ . The sampling process on the four input analog pins is quasi-independent so each time constant should be considered by itself and, under worst-case circumstances, the errors may add.

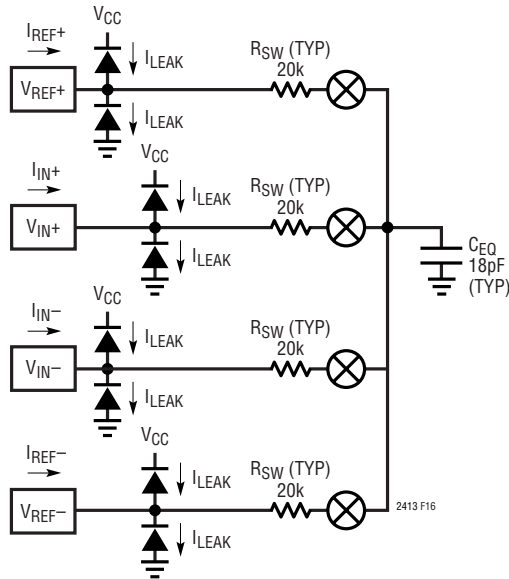
When using the internal oscillator ( $F_0 = \text{LOW}$ ), the LTC2413's front-end switched-capacitor network is clocked at 69900Hz corresponding to a 14.3 $\mu\text{s}$  sampling period. Thus, for settling errors of less than 1ppm, the driving source impedance should be chosen such that  $\tau \leq 14.3\mu\text{s}/14 = 1.02\mu\text{s}$ . When an external oscillator of frequency  $f_{EOSC}$  is used, the sampling period is  $2/f_{EOSC}$  and, for a settling error of less than 1ppm,  $\tau \leq 0.14/f_{EOSC}$ .

### Input Current

If complete settling occurs on the input, conversion results will be unaffected by the dynamic input current. An incomplete settling of the input signal sampling process may result in gain and offset errors, but it will not degrade the INL performance of the converter. Figure 16 shows the mathematical expressions for the average bias currents flowing through the IN<sup>+</sup> and IN<sup>-</sup> pins as a result of the sampling charge transfers when integrated over a substantial time period (longer than 64 internal clock cycles).



# APPLICATIONS INFORMATION



SWITCHING FREQUENCY  
 $f_{SW} = 69900\text{Hz}$  INTERNAL OSCILLATOR  
 $f_{SW} = 0.5 \cdot f_{EOSC}$  EXTERNAL OSCILLATOR

$$I(IN^+)_{AVG} = \frac{V_{IN} + V_{INCM} - V_{REFCM}}{0.5 \cdot R_{EQ}}$$

$$I(IN^-)_{AVG} = \frac{-V_{IN} + V_{INCM} - V_{REFCM}}{0.5 \cdot R_{EQ}}$$

$$I(REF^+)_{AVG} = \frac{1.5 \cdot V_{REF} - V_{INCM} + V_{REFCM}}{0.5 \cdot R_{EQ}} - \frac{V_{IN}^2}{V_{REF} \cdot R_{EQ}}$$

$$I(REF^-)_{AVG} = \frac{-1.5 \cdot V_{REF} - V_{INCM} + V_{REFCM}}{0.5 \cdot R_{EQ}} + \frac{V_{IN}^2}{V_{REF} \cdot R_{EQ}}$$

where:

$$V_{REF} = REF^+ - REF^-$$

$$V_{REFCM} = \left( \frac{REF^+ + REF^-}{2} \right)$$

$$V_{IN} = IN^+ - IN^-$$

$$V_{INCM} = \left( \frac{IN^+ - IN^-}{2} \right)$$

$R_{EQ} = 3.97\text{M}\Omega$  INTERNAL OSCILLATOR  
 $R_{EQ} = (0.555 \cdot 10^{12}) / f_{EOSC}$  EXTERNAL OSCILLATOR

Figure 16. LTC2413 Equivalent Analog Input Circuit

The effect of this input dynamic current can be analyzed using the test circuit of Figure 17. The  $C_{PAR}$  capacitor includes the LTC2413 pin capacitance (5pF typical) plus the capacitance of the test fixture used to obtain the results shown in Figures 18 and 19. A careful implementation can bring the total input capacitance ( $C_{IN} + C_{PAR}$ ) closer to 5pF thus achieving better performance than the one predicted by Figures 18 and 19. For simplicity, two distinct situations can be considered.

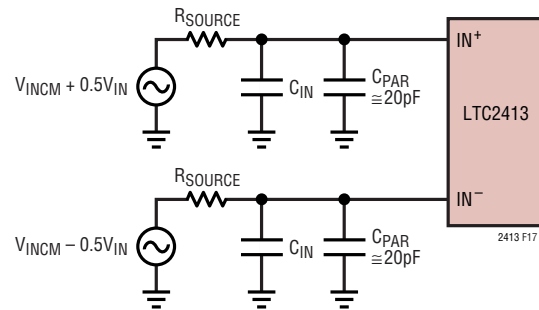


Figure 17. An RC Network at IN+ and IN-

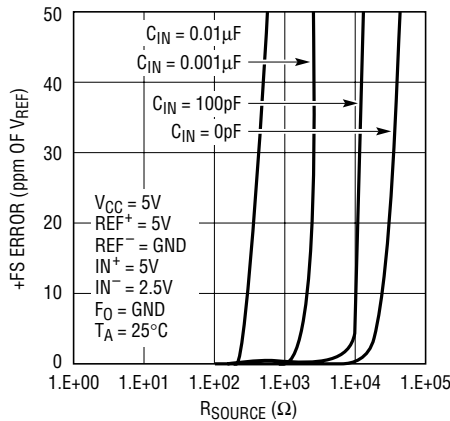


Figure 18. +FS Error vs  $R_{SOURCE}$  at  $IN^+$  or  $IN^-$  (Small  $C_{IN}$ )

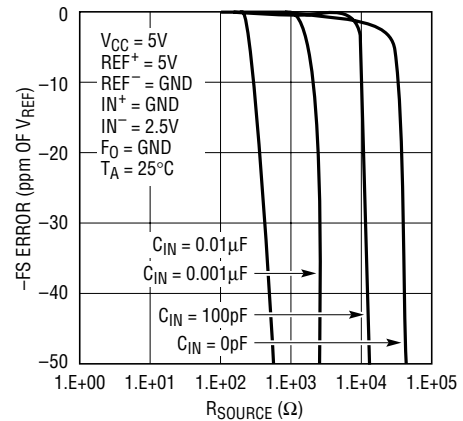


Figure 19. -FS Error vs  $R_{SOURCE}$  at  $IN^+$  or  $IN^-$  (Small  $C_{IN}$ )

## APPLICATIONS INFORMATION

For relatively small values of input capacitance ( $C_{IN} < 0.01\mu\text{F}$ ), the voltage on the sampling capacitor settles almost completely and relatively large values for the source impedance result in only small errors. Such values for  $C_{IN}$  will deteriorate the converter offset and gain performance without significant benefits of signal filtering and the user is advised to avoid them. Nevertheless, when small values of  $C_{IN}$  are unavoidably present as parasitics of input multiplexers, wires, connectors or sensors, the LTC2413 can maintain its exceptional accuracy while operating with relative large values of source resistance as shown in Figures 18 and 19. These measured results may be slightly different from the first order approximation suggested earlier because they include the effect of the actual second order input network together with the non-linear settling process of the input amplifiers. For small  $C_{IN}$  values, the settling on  $IN^+$  and  $IN^-$  occurs almost independently and there is little benefit in trying to match the source impedance for the two pins.

Larger values of input capacitors ( $C_{IN} > 0.01\mu\text{F}$ ) may be required in certain configurations for antialiasing or general input signal filtering. Such capacitors will average the input sampling charge and the external source resistance will see a quasi constant input differential impedance. When internal oscillator is used ( $F_0 = \text{LOW}$ ), the typical differential input resistance is  $2M\Omega$  which will generate a gain error of approximately 0.25ppm for each ohm of source resistance driving  $IN^+$  or  $IN^-$ . When  $F_0$  is driven by an external oscillator with a frequency  $f_{EOSC}$  (external conversion clock operation), the typical differential input resistance is  $0.28 \cdot 10^{12}/f_{EOSC}\Omega$  and each ohm of source resistance driving  $IN^+$  or  $IN^-$  will result in  $1.78 \cdot 10^{-6} \cdot f_{EOSC}\text{ppm}$  gain error. The effect of the source resistance on the two input pins is additive with respect to this gain error. The typical +FS and -FS errors as a function of the sum of the source resistance seen by  $IN^+$  and  $IN^-$  for large values of  $C_{IN}$  are shown in Figures 20 and 21.

In addition to this gain error, an offset error term may also appear. The offset error is proportional with the mismatch between the source impedance driving the two input pins  $IN^+$  and  $IN^-$  and with the difference between the input and reference common mode voltages. While the input drive circuit nonzero source impedance combined with the

converter average input current will not degrade the INL performance, indirect distortion may result from the modulation of the offset error by the common mode component of the input signal. Thus, when using large  $C_{IN}$  capacitor values, it is advisable to carefully match the source impedance seen by the  $IN^+$  and  $IN^-$  pins. When internal oscillator is used ( $F_0 = \text{LOW}$ ), every  $1\Omega$  mismatch in source impedance transforms a full-scale common mode input signal into a differential mode input signal of 0.25ppm. When  $F_0$  is driven by an external oscillator with a frequency  $f_{EOSC}$ , every  $1\Omega$  mismatch in source impedance transforms a full-scale common mode input signal into a differential mode input signal of  $1.78 \cdot 10^{-6} \cdot f_{EOSC}\text{ppm}$ . Figure 22 shows the typical offset error due to input common mode voltage for various values of source resistance imbalance between the  $IN^+$  and  $IN^-$  pins when large  $C_{IN}$  values are used.

If possible, it is desirable to operate with the input signal common mode voltage very close to the reference signal common mode voltage as is the case in the ratiometric measurement of a symmetric bridge. This configuration eliminates the offset error caused by mismatched source impedances.

The magnitude of the dynamic input current depends upon the size of the very stable internal sampling capacitors and upon the accuracy of the converter sampling clock. The accuracy of the internal clock over the entire temperature and power supply range is typical better than 0.5%. Such a specification can also be easily achieved by an external clock. When relatively stable resistors (50ppm/ $^{\circ}\text{C}$ ) are used for the external source impedance seen by  $IN^+$  and  $IN^-$ , the expected drift of the dynamic current, offset and gain errors will be insignificant (about 1% of their respective values over the entire temperature and voltage range). Even for the most stringent applications a one-time calibration operation may be sufficient.

In addition to the input sampling charge, the input ESD protection diodes have a temperature dependent leakage current. This current, nominally 1nA ( $\pm 10\text{nA max}$ ), results in a small offset shift. A  $100\Omega$  source resistance will create a 0.1 $\mu\text{V}$  typical and 1 $\mu\text{V}$  maximum offset voltage.

## APPLICATIONS INFORMATION

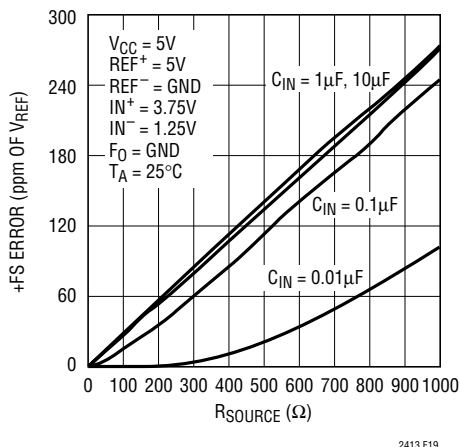


Figure 20. +FS Error vs  $R_{SOURCE}$  at  $IN^+$  or  $IN^-$  (Large  $C_{IN}$ )

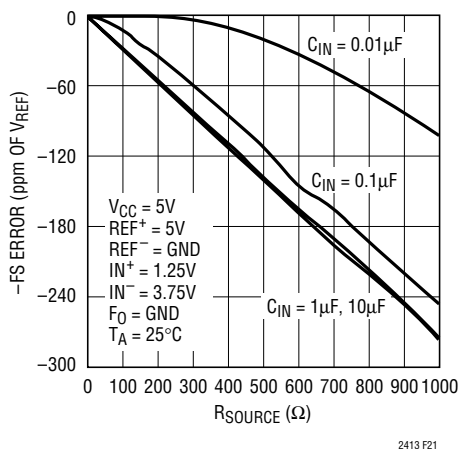


Figure 21. -FS Error vs  $R_{SOURCE}$  at  $IN^+$  or  $IN^-$  (Large  $C_{IN}$ )

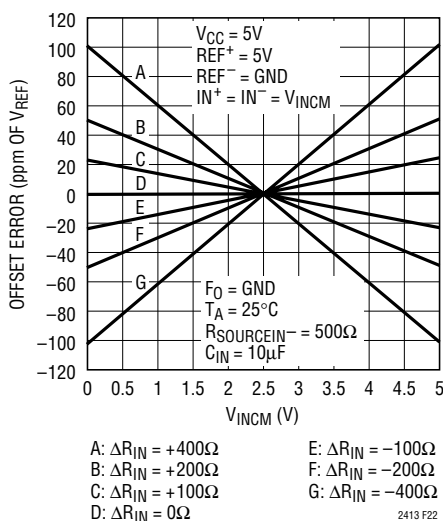


Figure 22. Offset Error vs Common Mode Voltage ( $V_{INCM} = IN^+ = IN^-$ ) and Input Source Resistance Imbalance ( $\Delta R_{IN} = R_{SOURCEIN^+} - R_{SOURCEIN^-}$ ) for Large  $C_{IN}$  Values ( $C_{IN} \geq 1\mu F$ )

### Reference Current

In a similar fashion, the LTC2413 samples the differential reference pins  $REF^+$  and  $REF^-$  transferring small amount of charge to and from the external driving circuits, thus produces a dynamic reference current. This current does not change the converter offset but it may degrade the gain and INL performance. The effect of this current can be analyzed in the same two distinct situations.

For relatively small values of the external reference capacitors ( $C_{REF} < 0.01\mu F$ ), the voltage on the sampling capacitor settles almost completely and relatively large values for the source impedance result in only small errors. Such values for  $C_{REF}$  will deteriorate the converter offset and gain performance without significant benefits of reference filtering and the user is advised to avoid them.

Larger values of reference capacitors ( $C_{REF} > 0.01\mu F$ ) may be required as reference filters in certain configurations. Such capacitors will average the reference sampling charge and the external source resistance will see a quasi constant reference differential impedance. When internal oscillator is used ( $F_O = LOW$ ), the typical differential input resistance is  $1.43M\Omega$  which will generate a gain error of approximately  $0.35ppm$  for each ohm of source resistance driving  $REF^+$  or  $REF^-$ . When  $F_O$  is driven by an external oscillator with a frequency  $f_{EOSC}$  (external conversion clock operation), the typical differential reference resistance is  $0.20 \cdot 10^{12}/f_{EOSC}\Omega$  and each ohm of source resistance driving  $REF^+$  or  $REF^-$  will result in  $2.47 \cdot 10^{-6} \cdot f_{EOSC}ppm$  gain error. The effect of the source resistance on the two reference pins is additive with respect to this gain error. The typical +FS and -FS errors for various combinations of source resistance seen by the  $REF^+$  and  $REF^-$  pins and external capacitance  $C_{REF}$  connected to these pins are shown in Figures 23, 24, 25 and 26.

In addition to this gain error, the converter INL performance is degraded by the reference source impedance. When internal oscillator is used ( $F_O = LOW$ ), every  $100\Omega$  of source impedance driving  $REF^+$  or  $REF^-$  translates into about  $1.2ppm$  additional INL error. When  $F_O$  is driven by an external oscillator with a frequency  $f_{EOSC}$ , every  $100\Omega$  of source resistance driving  $REF^+$  or  $REF^-$  translates into about  $8.73 \cdot 10^{-6} \cdot f_{EOSC}ppm$  additional INL error.

APPLICATIONS INFORMATION

Figure 27 shows the typical INL error due to the source resistance driving the REF+ or REF- pins when large CREF values are used. The effect of the source resistance on the two reference pins is additive with respect to this INL error. In general, matching of source impedance for the REF+ and REF- pins does not help the gain or the INL error. The user is thus advised to minimize the combined source impedance driving the REF+ and REF- pins rather than to try to match it.

The magnitude of the dynamic reference current depends upon the size of the very stable internal sampling capacitors and upon the accuracy of the converter sampling clock. The accuracy of the internal clock over the entire temperature and power supply range is typical better than

0.5%. Such a specification can also be easily achieved by an external clock. When relatively stable resistors (50ppm/°C) are used for the external source impedance seen by REF+ and REF-, the expected drift of the dynamic current gain error will be insignificant (about 1% of its value over the entire temperature and voltage range). Even for the most stringent applications, a one-time calibration operation may be sufficient.

In addition to the reference sampling charge, the reference pins ESD protection diodes have a temperature dependent leakage current. This leakage current, nominally 1nA (±10nA max), results in a small gain error. A 100Ω source resistance will create a 0.05μV typical and 0.5μV maximum full-scale error.

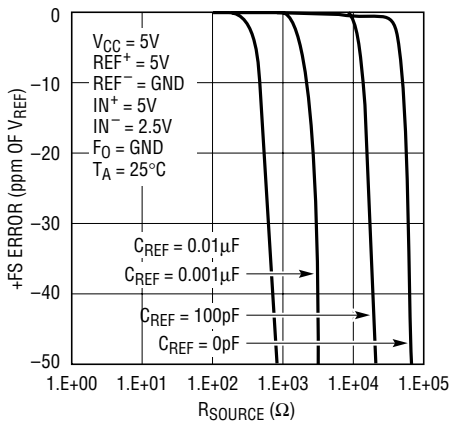


Figure 23. +FS Error vs R\_SOURCE at REF+ or REF- (Small C\_REF)

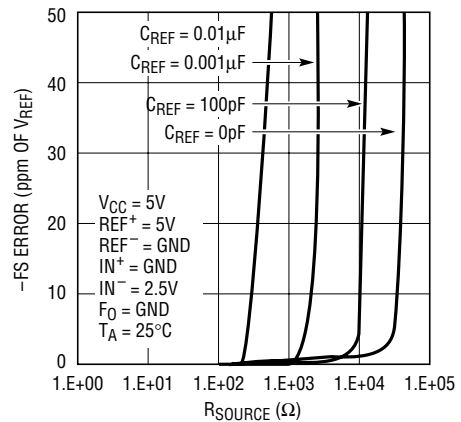


Figure 24. -FS Error vs R\_SOURCE at REF+ or REF- (Small C\_REF)

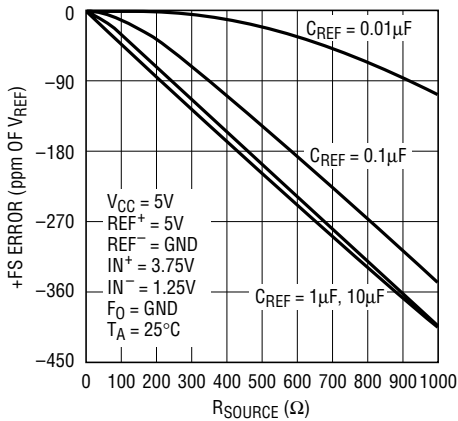


Figure 25. +FS Error vs R\_SOURCE at REF+ or REF- (Large C\_REF)

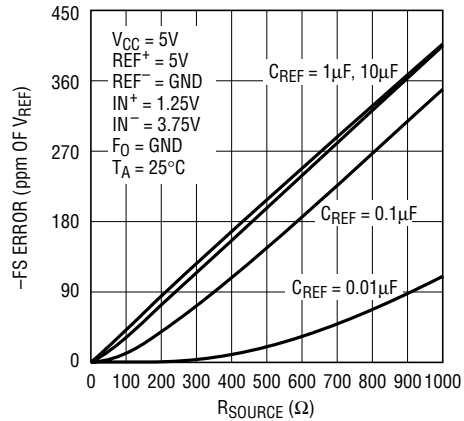
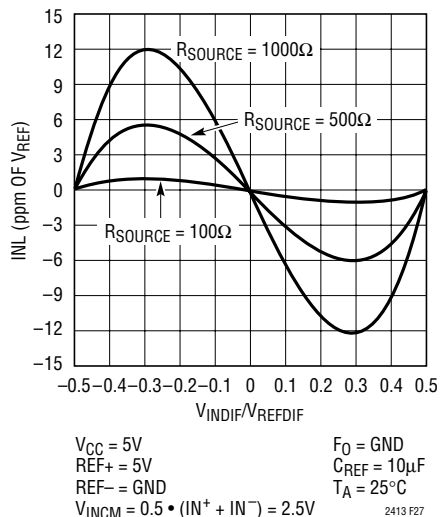


Figure 26. -FS Error vs R\_SOURCE at REF+ or REF- (Large C\_REF)

sn2413 2413fs

## APPLICATIONS INFORMATION



**Figure 27. INL vs Differential Input Voltage ( $V_{IN} = IN^+ - IN^-$ ) and Reference Source Resistance ( $R_{SOURCE}$  at  $REF^+$  and  $REF^-$  for Large  $C_{REF}$  Values ( $C_{REF} \geq 1\mu F$ )**

### Output Data Rate

When using its internal oscillator, the LTC2413 can produce up to 6.8 readings per second. The actual output data rate will depend upon the length of the sleep and data output phases which are controlled by the user and which can be made insignificantly short. When operated with an external conversion clock ( $F_O$  connected to an external oscillator), the LTC2413 output data rate can be increased as desired. The duration of the conversion phase is  $20510/f_{EOSC}$ . If  $f_{EOSC} = 139800\text{Hz}$ , the converter behaves as if the internal oscillator is used with simultaneous 50Hz/60Hz rejection. There is no significant difference in the LTC2413 performance between these two operation modes.

An increase in  $f_{EOSC}$  over the nominal 139800Hz will translate into a proportional increase in the maximum output data rate. This substantial advantage is nevertheless accompanied by three potential effects, which must be carefully considered.

First, a change in  $f_{EOSC}$  will result in a proportional change in the internal notch position and in a reduction of the converter differential mode rejection at the power-line frequency. In many applications, the subsequent performance degradation can be substantially reduced by relying upon the LTC2413's exceptional common mode rejection and by carefully eliminating common mode to differential mode conversion sources in the input circuit. The user should avoid single-ended input filters and should maintain a very high degree of matching and symmetry in the circuits driving the  $IN^+$  and  $IN^-$  pins.

Second, the increase in clock frequency will increase proportionally the amount of sampling charge transferred through the input and the reference pins. If large external input and/or reference capacitors ( $C_{IN}$ ,  $C_{REF}$ ) are used, the previous section provides formulae for evaluating the effect of the source resistance upon the converter performance for any value of  $f_{EOSC}$ . If small external input and/or reference capacitors ( $C_{IN}$ ,  $C_{REF}$ ) are used, the effect of the external source resistance upon the LTC2413 typical performance can be inferred from Figures 18, 19, 23 and 24 in which the horizontal axis is scaled by  $139800/f_{EOSC}$ .

## APPLICATIONS INFORMATION

Third, an increase in the frequency of the external oscillator above 460800Hz (a more than 3× increase in the output data rate) will start to decrease the effectiveness of the internal autocalibration circuits. This will result in a progressive degradation in the converter accuracy and linearity. Typical measured performance curves for output data rates up to 100 readings per second are shown in Fig-

ures 28 through 35, inclusive. In order to obtain the highest possible level of accuracy from this converter at output data rates above 20 readings per second, the user is advised to maximize the power supply voltage used and to limit the maximum ambient operating temperature. In certain circumstances, a reduction of the differential reference voltage may be beneficial.

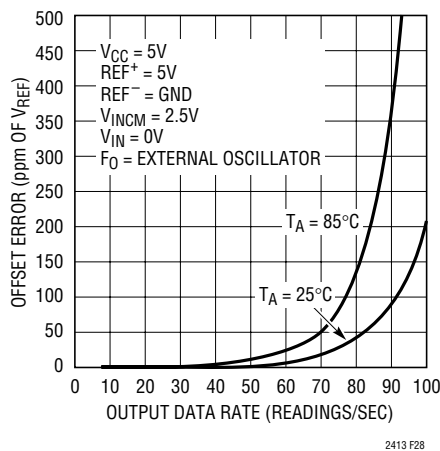


Figure 28. Offset Error vs Output Data Rate and Temperature

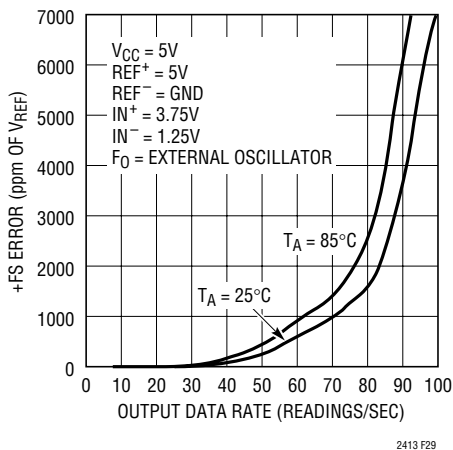


Figure 29. +FS Error vs Output Data Rate and Temperature

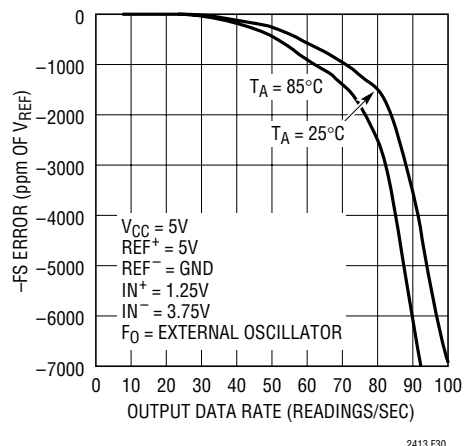
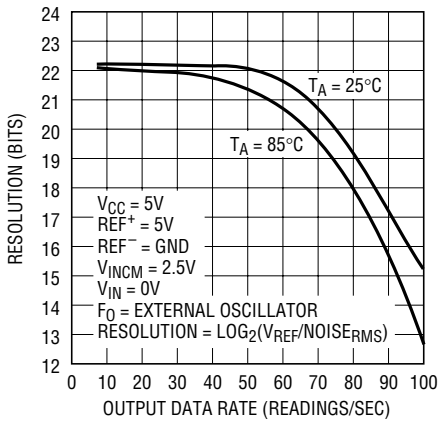


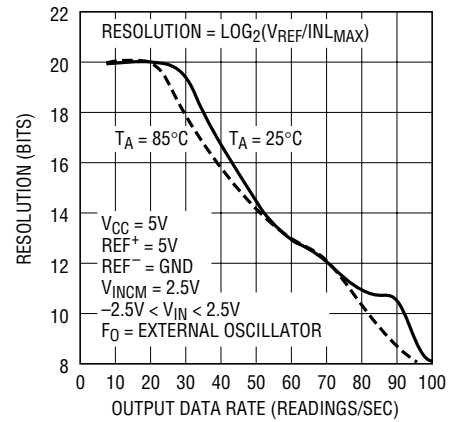
Figure 30. -FS Error vs Output Data Rate and Temperature

# APPLICATIONS INFORMATION



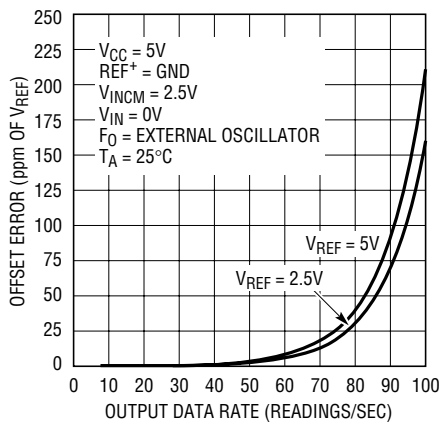
2413 F31

**Figure 31. Resolution ( $\text{Noise}_{\text{RMS}} \leq 1\text{LSB}$ ) vs Output Data Rate and Temperature**



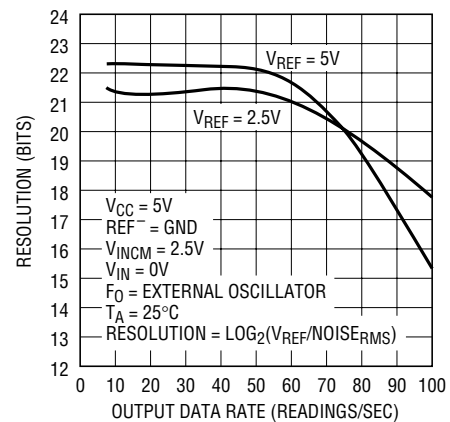
2413 F32

**Figure 32. Resolution ( $\text{INL}_{\text{RMS}} \leq 1\text{LSB}$ ) vs Output Data Rate and Temperature**



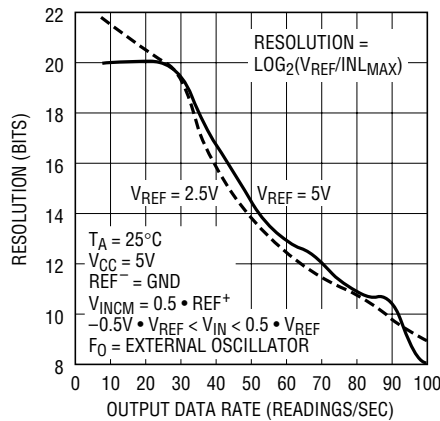
2413 F33

**Figure 33. Offset Error vs Output Data Rate and Reference Voltage**



2413 F34

**Figure 34. Resolution ( $\text{Noise}_{\text{RMS}} \leq 1\text{LSB}$ ) vs Output Data Rate and Reference Voltage**



2413 F35

**Figure 35. Resolution ( $\text{INL}_{\text{MAX}} \leq 1\text{LSB}$ ) vs Output Data Rate and Reference Voltage**

## APPLICATIONS INFORMATION

### Input Bandwidth

The combined effect of the internal sinc<sup>4</sup> digital filter and of the analog and digital autocalibration circuits determines the LTC2413 input bandwidth. When the internal oscillator is used ( $F_0 = \text{LOW}$ ), the 3dB input bandwidth is 3.3Hz. If an external conversion clock generator of frequency  $f_{\text{EOSC}}$  is connected to the  $F_0$  pin, the 3dB input bandwidth is  $0.236 \cdot 10^{-6} \cdot f_{\text{EOSC}}$ .

Due to the complex filtering and calibration algorithms utilized, the converter input bandwidth is not modeled very accurately by a first order filter with the pole located at the 3dB frequency. When the internal oscillator is used, the shape of the LTC2413 input bandwidth is shown in Figure 36. When an external oscillator of frequency  $f_{\text{EOSC}}$  is used, the shape of the LTC2413 input bandwidth can be derived from Figure 36, in which the horizontal axis is scaled by  $f_{\text{EOSC}}/139800$ .

The conversion noise (800nV<sub>RMS</sub> typical for  $V_{\text{REF}} = 5\text{V}$ ) can be modeled as a white noise source connected to a noise free converter. The noise spectral density is 63nV/ $\sqrt{\text{Hz}}$  for an infinite bandwidth source and 77nV/ $\sqrt{\text{Hz}}$  for a single 0.5MHz pole source. From these numbers, it is clear that particular attention must be given to the design of external amplification circuits. Such circuits face the simultaneous requirements of very low bandwidth (just a few Hz) in order to reduce the output referred noise and relatively high bandwidth (at least 500kHz) necessary to drive the input switched-capacitor network. A possible solution is a

high gain, low bandwidth amplifier stage followed by a high bandwidth unity-gain buffer.

When external amplifiers are driving the LTC2413, the ADC input referred system noise calculation can be simplified by Figure 37. The noise of an amplifier driving the LTC2413 input pin can be modeled as a band limited white noise source. Its bandwidth can be approximated by the bandwidth of a single pole lowpass filter with a corner frequency  $f_i$ . The amplifier noise spectral density is  $n_i$ . From Figure 37, using  $f_i$  as the x-axis selector, we can find on the y-axis the noise equivalent bandwidth  $\text{freq}_i$  of the input driving amplifier. This bandwidth includes the band limiting effects of the ADC internal calibration and filtering. The noise of the driving amplifier referred to the converter input and including all these effects can be calculated as  $N = n_i \cdot \sqrt{\text{freq}_i}$ . The total system noise (referred to the LTC2413 input) can now be obtained by summing as square root of sum of squares the three ADC input referred noise sources: the LTC2413 internal noise (800nV), the noise of the  $\text{IN}^+$  driving amplifier and the noise of the  $\text{IN}^-$  driving amplifier.

If the  $F_0$  pin is driven by an external oscillator of frequency  $f_{\text{EOSC}}$ , Figure 37 can still be used for noise calculation if the x-axis is scaled by  $f_{\text{EOSC}}/139800$ . For large values of the ratio  $f_{\text{EOSC}}/139800$ , the Figure 37 plot accuracy begins to decrease, but in the same time the LTC2413 noise floor rises and the noise contribution of the driving amplifiers lose significance.

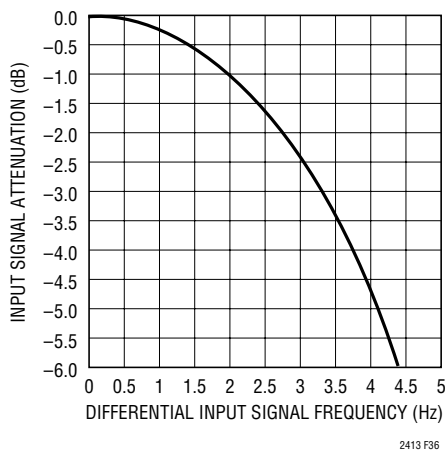


Figure 36. Input Signal Bandwidth Using the Internal Oscillator

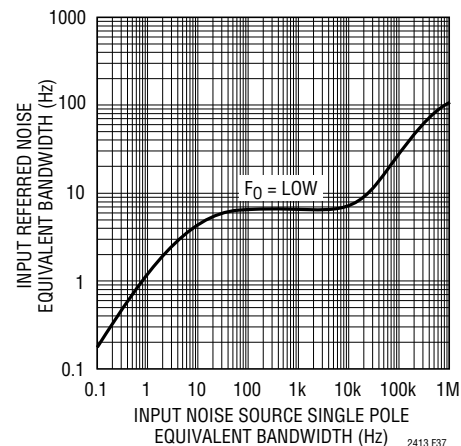


Figure 37. Input Referred Noise Equivalent Bandwidth of an Input Connected White Noise Source

sn2413 2413fs



## APPLICATIONS INFORMATION

### Normal Mode Rejection and Antialiasing

One of the advantages delta-sigma ADCs offer over conventional ADCs is on-chip digital filtering. Combined with a large oversampling ratio, the LTC2413 significantly simplifies antialiasing filter requirements.

The sinc<sup>4</sup> digital filter provides greater than 120dB normal mode rejection at all frequencies except DC and integer multiples of the modulator sampling frequency ( $f_S$ ). The LTC2413's autocalibration circuits further simplify the antialiasing requirements by additional normal mode signal filtering both in the analog and digital domain. Independent of the operating mode,  $f_S = 256 \cdot f_N = 2048 \cdot f_{OUTMAX}$  where  $f_N$  is the notch frequency and  $f_{OUTMAX}$  is

the maximum output data rate. In the internal oscillator mode,  $f_S = 13980\text{Hz}$ . In the external oscillator mode,  $f_S = f_{EOSC}/10$ .

The combined normal mode rejection performance is shown in Figure 38. The regions of low rejection occurring at integer multiples of  $f_S$  have a very narrow bandwidth. Magnified details of the normal mode rejection curves are shown in Figure 39 (rejection near DC) and Figure 40 (rejection at  $f_S = 256f_N$ ) where  $f_N$  represents the notch frequency. These curves have been derived for the external oscillator mode but they can be used in all operating modes by appropriately selecting the  $f_N$  value.

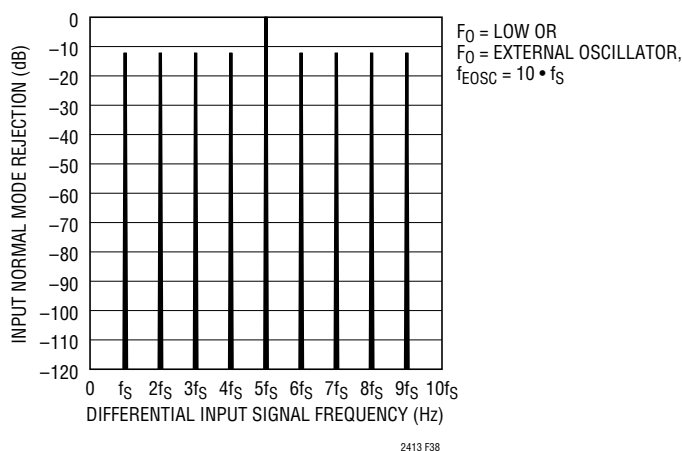


Figure 38. Input Normal Mode Rejection

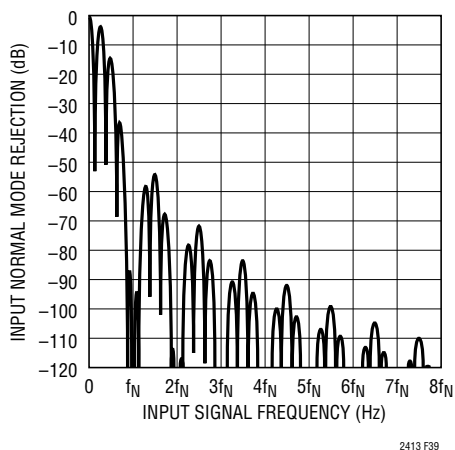


Figure 39. Input Normal Mode Rejection

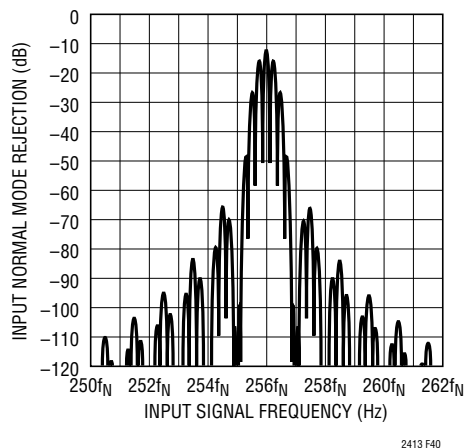


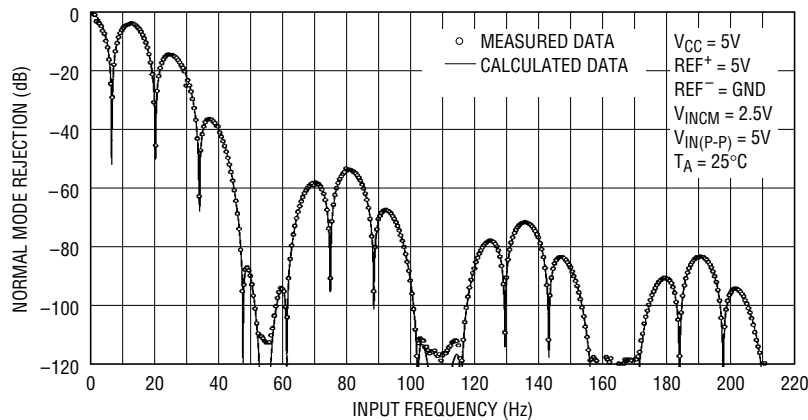
Figure 40. Input Normal Mode Rejection

## APPLICATIONS INFORMATION

The user can expect to achieve in practice this level of performance using the internal oscillator, as it is demonstrated by Figure 41. Typical measured values of the normal mode rejection of the LTC2413 operating with the internal oscillator are shown in Figure 41 superimposed over the theoretical calculated curve.

As a result of these remarkable normal mode specifications, minimal (if any) antialias filtering is required in front of the LTC2413. If passive RC components are placed in front of the LTC2413, the input dynamic current should be considered (see Input Current section). In cases where large effective RC time constants are used, an external buffer amplifier may be required to minimize the effects of dynamic input current.

Traditional high order delta-sigma modulators, while providing very good linearity and resolution, suffer from potential instabilities at large input signal levels. The proprietary architecture used for the LTC2413 third order modulator resolves this problem and guarantees a predictable stable behavior at input signal levels of up to 150% of full scale. In many industrial applications, it is not uncommon to have to measure microvolt level signals superimposed over volt level perturbations and LTC2413 is eminently suited for such tasks. When the perturbation is differential, the specification of interest is the normal mode rejection for large input signal levels. With a reference voltage  $V_{REF} = 5V$ , the LTC2413 has a full-scale differential input



2413 F41

**Figure 41. Input Normal Mode Rejection vs Input Frequency with Input Perturbation of 100% of Full Scale**

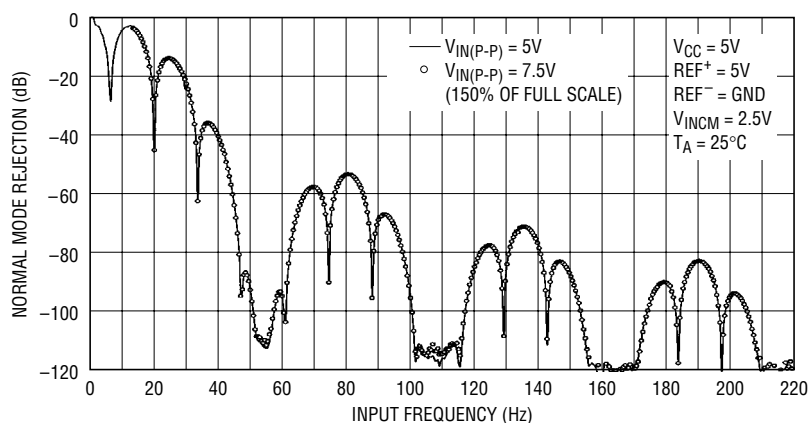
## APPLICATIONS INFORMATION

range of 5V peak-to-peak. Figure 42 shows measurement results for the LTC2413 normal mode rejection ratio with a 7.5V peak-to-peak (150% of full scale) input signal superimposed over the more traditional normal mode rejection ratio results obtained with a 5V peak-to-peak (full scale) input signal. It is clear that the LTC2413 rejection performance is maintained with no compromises in this extreme situation. When operating with large input signal levels, the user must observe that such signals do not violate the device's absolute maximum ratings.

### BRIDGE APPLICATIONS

Typical strain gauge based bridges deliver only 2mV/Volt of excitation. As the maximum reference voltage of the LTC2413 is 5V, remote sensing of applied excitation without additional circuitry requires that excitation be

limited to 5V. This gives only 10mV full scale, which can be resolved to 1 part in 10000 without averaging. For many solid state sensors, this is still better than the sensor. For example, averaging 64 samples however reduces the noise level by a factor of eight, bringing the resolving power to 1 part in 80000, comparable to better weighing systems. Hysteresis and creep effects in the load cells are typically much greater than this. Most applications that require strain measurements to this level of accuracy are measuring slowly changing phenomena, hence the time required to average a large number of readings is usually not an issue. For those systems that require accurate measurement of a small incremental change on a significant tare weight, the lack of history effects in the LTC2400 family is of great benefit.



2413 F42

**Figure 42. Measured Input Normal Mode Rejection vs Input Frequency with Input Perturbation of 150% of Full Scale**

## APPLICATIONS INFORMATION

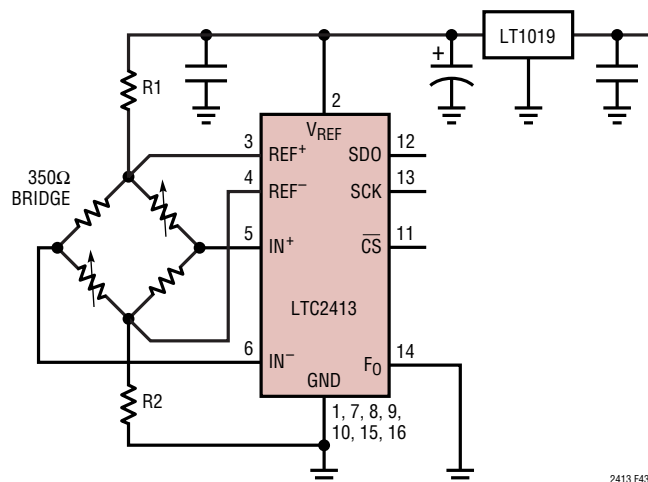
For those applications that cannot be fulfilled by the LTC2413 alone, compensating for error in external amplification can be done effectively due to the “no latency” feature of the LTC2413. No latency operation allows samples of the amplifier offset and gain to be interleaved with weighing measurements. The use of correlated double sampling allows suppression of  $1/f$  noise, offset and thermocouple effects within the bridge. Correlated double sampling involves alternating the polarity of excitation and dealing with the reversal of input polarity mathematically. Alternatively, bridge excitation can be increased to as much as  $\pm 10V$ , if one of several precision attenuation techniques is used to produce a precision divide operation on the reference signal. Another option is the use of a reference within the 5V input range of the LTC2413 and developing excitation via fixed gain, or LTC1043 based voltage multiplication, along with remote feedback in the excitation amplifiers, as shown in Figures 48 and 50.

Figure 43 shows an example of a simple bridge connection. Note that it is suitable for any bridge application where measurement speed is not of the utmost importance. For many applications where large vessels are weighed, the average weight over an extended period of time is of concern and short term weight is not readily determined due to movement of contents, or mechanical resonance. Often, large weighing applications involve load

cells located at each load bearing point, the output of which can be summed passively prior to the signal processing circuitry, actively with amplification prior to the ADC, or can be digitized via multiple ADC channels and summed mathematically. The mathematical summation of the output of multiple LTC2413's provides the benefit of a root square reduction in noise. The low power consumption of the LTC2413 makes it attractive for multidrop communication schemes where the ADC is located within the load-cell housing.

A direct connection to a load cell is perhaps best incorporated into the load-cell body, as minimizing the distance to the sensor largely eliminates the need for protection devices, RFI suppression and wiring. The LTC2413 exhibits extremely low temperature dependent drift. As a result, exposure to external ambient temperature ranges does not compromise performance. The incorporation of any amplification considerably complicates thermal stability, as input offset voltages and currents, temperature coefficient of gain settling resistors all become factors.

The circuit in Figure 44 shows an example of a simple amplification scheme. This example produces a differential output with a common mode voltage of 2.5V, as determined by the bridge. The use of a true three amplifier instrumentation amplifier is not necessary, as the LTC2413



R1 AND R2 CAN BE USED TO INCREASE TOLERABLE AC COMPONENT ON REF SIGNALS

Figure 43. Simple Bridge Connection

## APPLICATIONS INFORMATION

has common mode rejection far beyond that of most amplifiers. The LTC1051 is a dual autozero amplifier that can be used to produce a gain of 15 before its input referred noise dominates the LTC2413 noise. This example shows a gain of 34, that is determined by a feedback network built using a resistor array containing 8 individual resistors. The resistors are organized to optimize temperature tracking in the presence of thermal gradients. The second LTC1051 buffers the low noise input stage from the transient load steps produced during conversion.

The gain stability and accuracy of this approach is very good, due to a statistical improvement in resistor matching due to individual error contribution being reduced. A gain of 34 may seem low, when compared to common practice in earlier generations of load-cell interfaces, however the accuracy of the LTC2413 changes the rationale. Achieving high gain accuracy and linearity at higher gains may prove difficult, while providing little benefit in terms of noise reduction.

At a gain of 100, the gain error that could result from typical open-loop gain of 160dB is  $-1\text{ppm}$ , however, worst-case is at the minimum gain of 116dB, giving a gain error of  $-158\text{ppm}$ . Worst-case gain error at a gain of 34, is  $-54\text{ppm}$ . The use of the LTC1051A reduces the worst-case gain error to  $-33\text{ppm}$ . The advantage of gain higher than 34, then becomes dubious, as the input referred noise sees little improvement<sup>1</sup> and gain accuracy is potentially compromised.

Note that this 4-amplifier topology has advantages over the typical integrated 3-amplifier instrumentation amplifier in that it does not have the high noise level common in the output stage that usually dominates when an instrumentation amplifier is used at low gain. If this amplifier is used at a gain of 10, the gain error is only  $10\text{ppm}$  and input referred noise is reduced to  $0.1\mu\text{V}_{\text{RMS}}$ . The buffer stages can also be configured to provide gain of up to 50 with high gain stability and linearity.

Figure 45 shows an example of a single amplifier used to produce single-ended gain. This topology is best used in applications where the gain setting resistor can be made to match the temperature coefficient of the strain gauges. If the bridge is composed of precision resistors, with only one or two variable elements, the reference arm of the bridge can be made to act in conjunction with the feedback resistor to determine the gain. If the feedback resistor is incorporated into the design of the load cell, using resistors which match the temperature coefficient of the load-cell elements, good results can be achieved without the need for resistors with a high degree of absolute accuracy. The common mode voltage in this case, is again a function of the bridge output. Differential gain as used with a  $350\Omega$  bridge is  $A_V = (R1 + R2)/(R1 + 175\Omega)$ . Common mode gain is half the differential gain. The maximum differential signal that can be used is  $1/4 V_{\text{REF}}$ , as opposed to  $1/2 V_{\text{REF}}$  in the 2-amplifier topology above.

### Remote Half Bridge Interface

As opposed to full bridge applications, typical half bridge applications must contend with nonlinearity in the bridge output, as signal swing is often much greater. Applications include RTD's, thermistors and other resistive elements that undergo significant changes over their span. For single variable element bridges, the nonlinearity of the half bridge output can be eliminated completely; if the reference arm of the bridge is used as the reference to the ADC, as shown in Figure 46. The LTC2413 can accept inputs up to  $1/2 V_{\text{REF}}$ . Hence, the reference resistor R1 must be at least  $2\times$  the highest value of the variable resistor.

In the case of  $100\Omega$  platinum RTD's, this would suggest a value of  $800\Omega$  for R1. Such a low value for R1 is not advisable due to self-heating effects. A value of  $25.5\text{k}$  is shown for R1, reducing self-heating effects to acceptable levels for most sensors.

<sup>1</sup>Input referred noise for  $A_V = 34$  for approximately  $0.05\mu\text{V}_{\text{RMS}}$ , whereas at a gain of 50, it would be  $0.048\mu\text{V}_{\text{RMS}}$ .

**APPLICATIONS INFORMATION**

The basic circuit shown in Figure 46 shows connections for a full 4-wire connection to the sensor, which may be located remotely. The differential input connections will reject induced or coupled 60Hz interference, however, the reference inputs do not have the same rejection. If 60Hz or other noise is present on the reference input, a low pass filter is recommended as shown in Figure 47. Note that you cannot place a large capacitor directly at the junction of R1 and R2, as it will store charge from the sampling process. A better approach is to produce a low pass filter decoupled from the input lines with a high value resistor (R3).

The use of a third resistor in the half bridge, between the variable and fixed elements gives essentially the same result as the two resistor version, but has a few benefits. If, for example, a 25k reference resistor is used to set the excitation current with a 100Ω RTD, the negative reference input is sampling the same external node as the positive input, but may result in errors if used with a long cable. For short cable applications, the errors may be acceptably low. If instead the single 25k resistor is replaced with a 10k 5% and a 10k 0.1% reference resistor, the noise level introduced at the reference, at least at

higher frequencies, will be reduced. A filter can be introduced into the network, in the form of one or more capacitors, or ferrite beads, as long as the sampling pulses are not translated into an error. The reference voltage is also reduced, but this is not undesirable, as it will decrease the value of the LSB, although, not the input referred noise level.

The circuit shown in Figure 47 shows a more rigorous example of Figure 46, with increased noise suppression and more protection for remote applications.

Figure 48 shows an example of gain in the excitation circuit and remote feedback from the bridge. The LTC1043's provide voltage multiplication, providing ±10V from a 5V reference with only 1ppm error. The amplifiers are used at unity-gain and, hence, introduce a very little error due to gain error or due to offset voltages. A 1μV/°C offset voltage drift translates into 0.05ppm/°C gain error. Simpler alternatives, with the amplifiers providing gain using resistor arrays for feedback, can produce results that are similar to bridge sensing schemes via attenuators. Note that the amplifiers must have high open-loop gain or gain error will

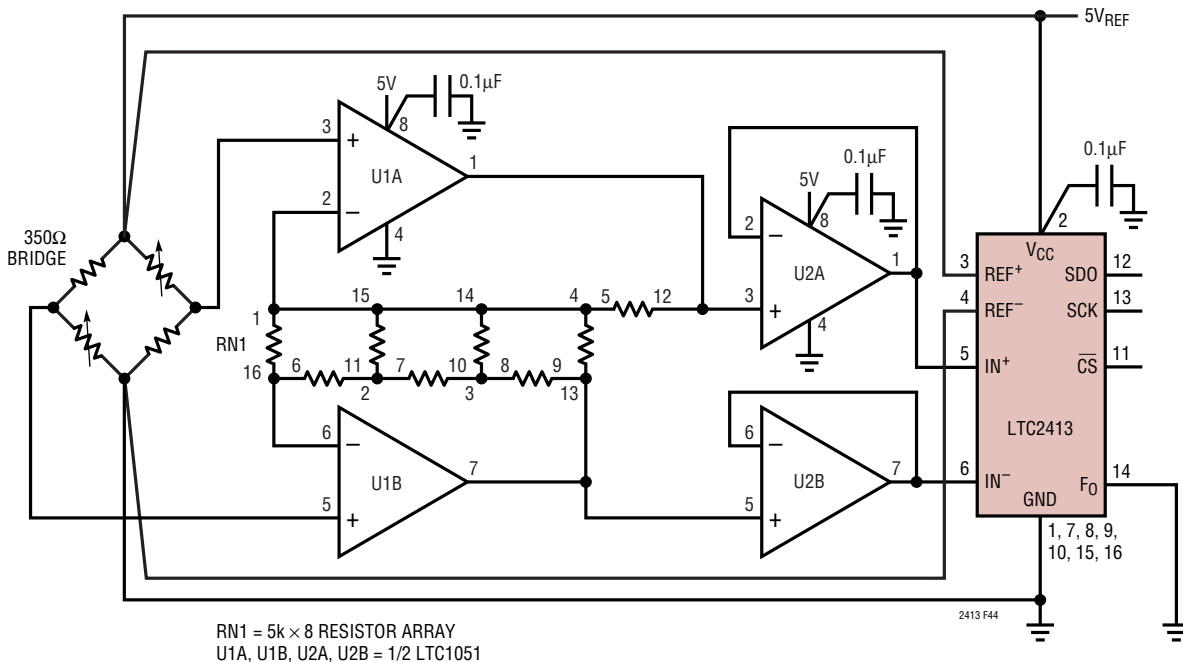


**Figure 44. Using Autozero Amplifiers to Reduce Input Referred Noise**

## APPLICATIONS INFORMATION

be a source of error. The fact that input offset voltage has relatively little effect on overall error may lead one to use low performance amplifiers for this application. Note that the gain of a device such as an LF156, (25V/mV over temperature) will produce a worst-case error of  $-180\text{ppm}$  at a noise gain of 3, such as would be encountered in an inverting gain of 2, to produce  $-10\text{V}$  from a  $5\text{V}$  reference.

The error associated with the  $10\text{V}$  excitation would be  $-80\text{ppm}$ . Hence, overall reference error could be as high as  $130\text{ppm}$ , the average of the two.

Figure 50 shows a similar scheme to provide excitation using resistor arrays to produce precise gain. The circuit is configured to provide  $10\text{V}$  and  $-5\text{V}$  excitation to the bridge, producing a common mode voltage at the input to the LTC2413 of  $2.5\text{V}$ , maximizing the AC input range for applications where induced  $60\text{Hz}$  could reach amplitudes up to  $2V_{\text{RMS}}$ .

The circuits in Figures 48 and 50 could be used where multiple bridge circuits are involved and bridge output can be multiplexed onto a single LTC2413, via an inexpensive multiplexer such as the 74HC4052.

Figure 49 shows the use of an LTC2413 with a differential multiplexer. This is an inexpensive multiplexer that will contribute some error due to leakage if used directly with the output from the bridge, or if resistors are inserted as a protection mechanism from overvoltage. Although the bridge output may be within the input range of the A/D and multiplexer in normal operation, some thought should be given to fault conditions that could result in full excitation voltage at the inputs to the multiplexer or ADC. The use of amplification prior to the multiplexer will largely eliminate errors associated with channel leakage developing error voltages in the source impedance.

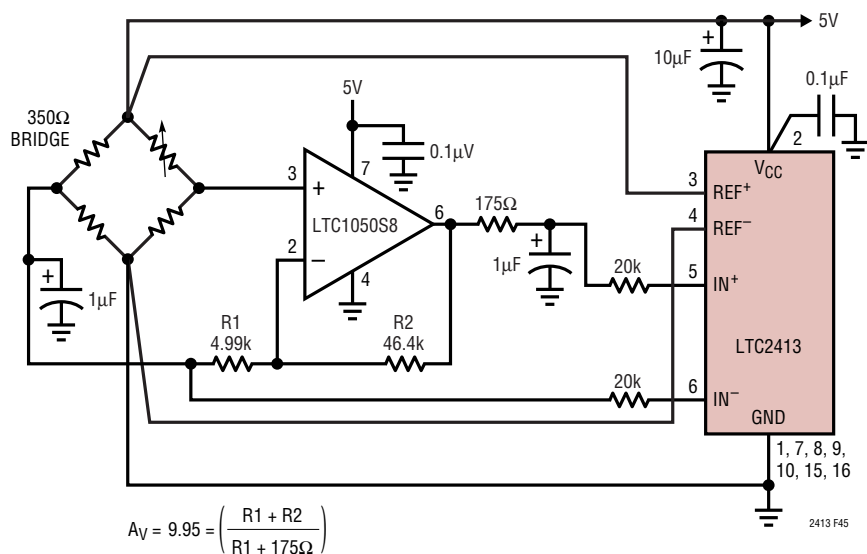


Figure 45. Bridge Amplification Using a Single Amplifier

## APPLICATIONS INFORMATION

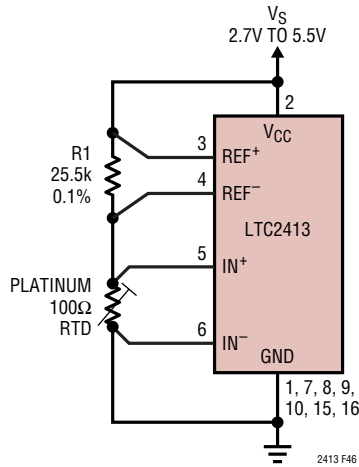


Figure 46. Remote Half Bridge Interface

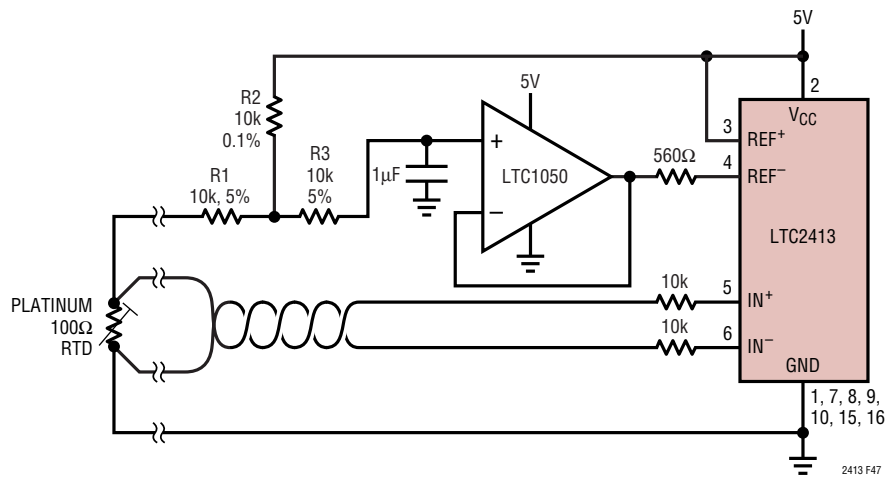


Figure 47. Remote Half Bridge Sensing with Noise Suppression on Reference



APPLICATIONS INFORMATION

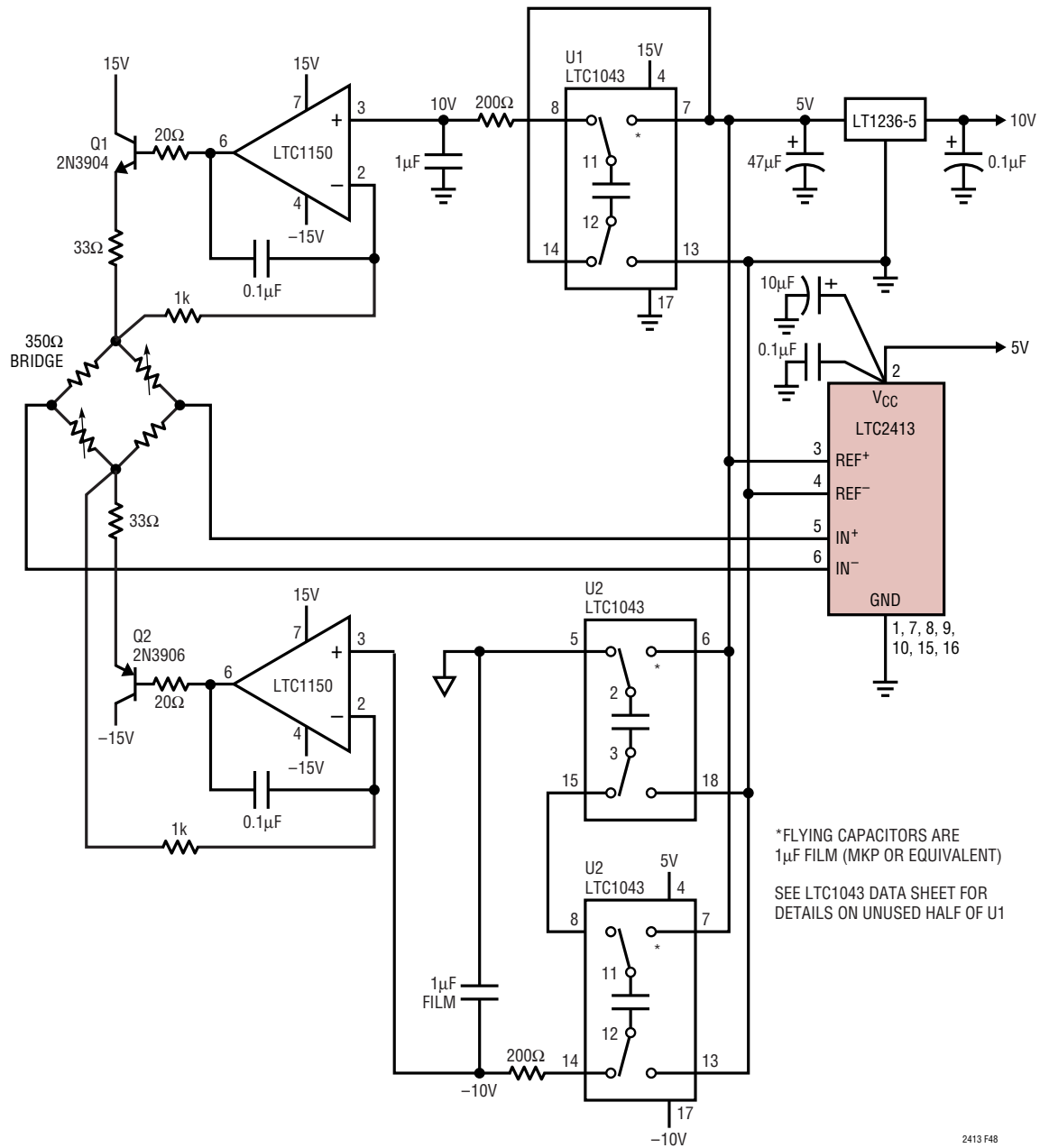


Figure 48. LTC1043 Provides Precise 4X Reference for Excitation Voltages

APPLICATIONS INFORMATION

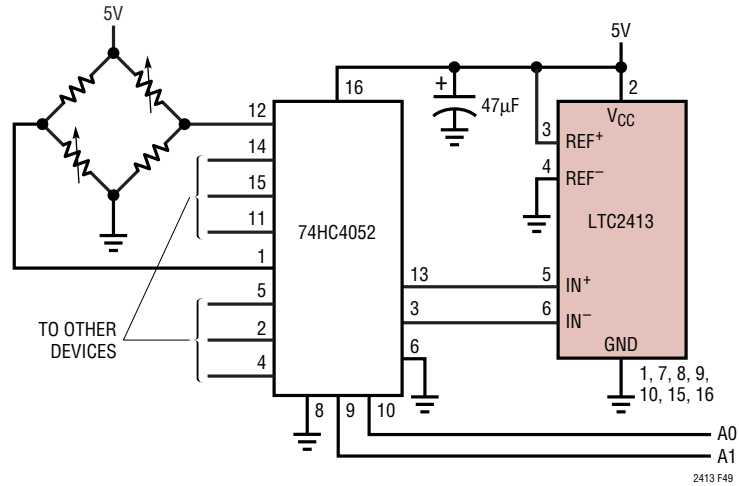
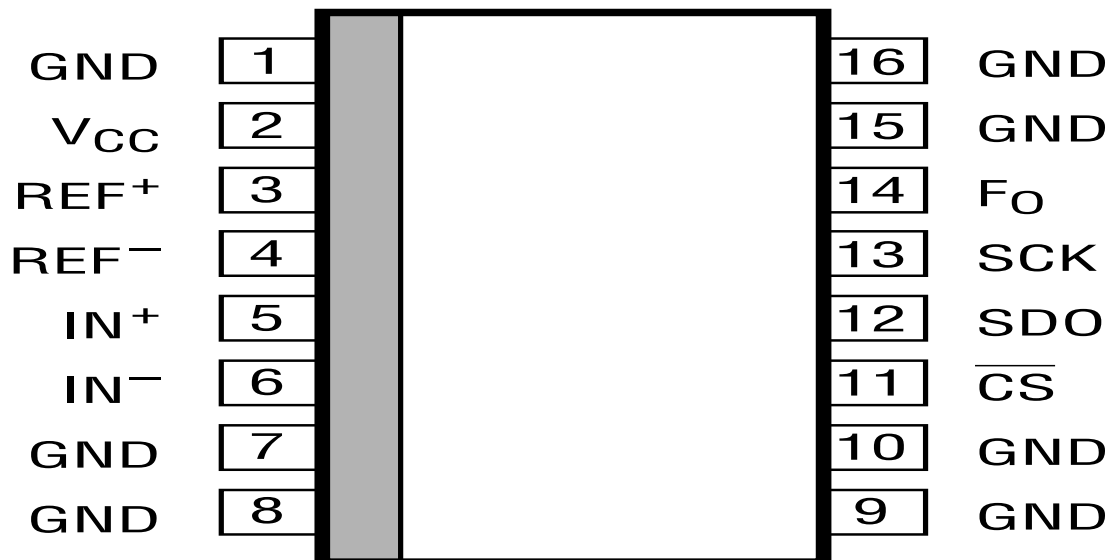


Figure 49. Use a Differential Multiplexer to Expand Channel Capability

## PACKAGE DESCRIPTION

GN Package  
 16-Lead Plastic SSOP (Narrow .150 Inch)  
 (Reference LTC DWG # 05-08-1641)

### TOP VIEW



GN PACKAGE  
 16-LEAD PLASTIC SSOP

TYPICAL APPLICATION

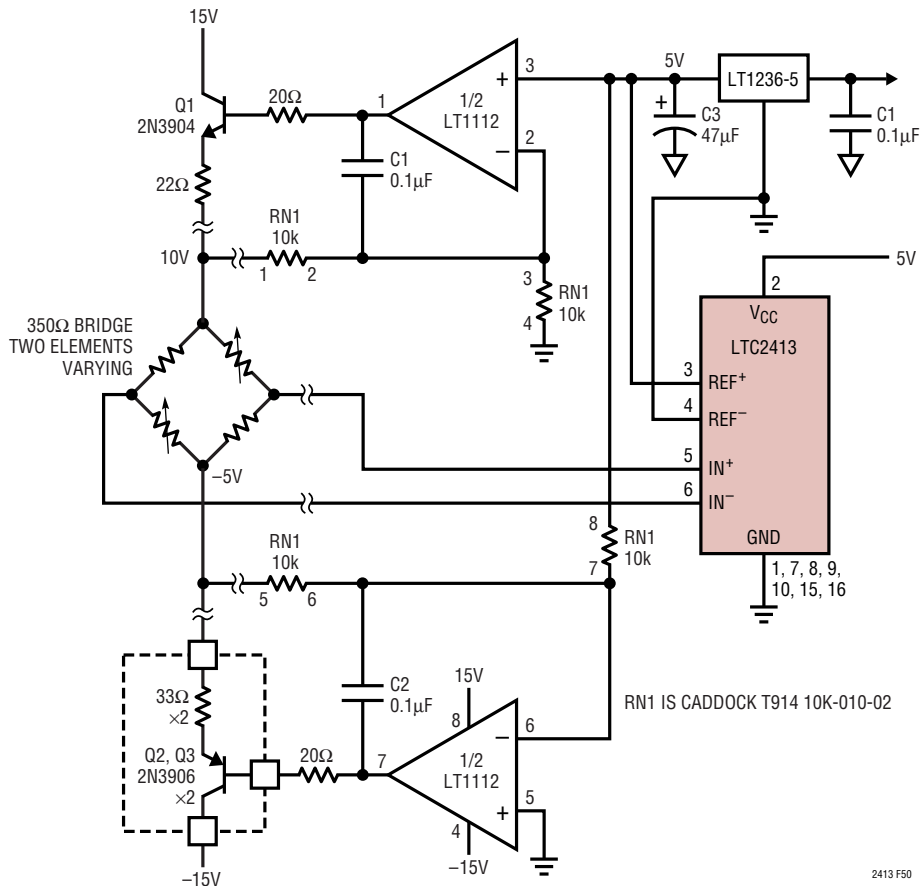


Figure 50. Use Resistor Arrays to Provide Precise Matching in Excitation Amplifier

RELATED PARTS

PART NUMBER	DESCRIPTION	COMMENTS
LT1019	Precision Bandgap Reference, 2.5V, 5V	3ppm/°C Drift, 0.05% Max Initial Accuracy
LT1025	Micropower Thermocouple Cold Junction Compensator	80μA Supply Current, 0.5°C Initial Accuracy
LTC1043	Dual Precision Instrumentation Switched Capacitor Building Block	Precise Charge, Balanced Switching, Low Power
LTC1050	Precision Chopper Stabilized Op Amp	No External Components 5μV Offset, 1.6μV <sub>p-p</sub> Noise
LT1236A-5	Precision Bandgap Reference, 5V	0.05% Max Initial Accuracy, 5ppm/°C Drift
LT1460	Micropower Series Reference	0.075% Max, 10ppm/°C Max Drift
LTC2400	24-Bit, No Latency ΔΣ ADC in SO-8	0.3ppm Noise, 4ppm INL, 10ppm Total Unadjusted Error, 200μA
LTC2401/LTC2402	1-/2-Channel, 24-Bit, No Latency ΔΣ ADC in MSOP	0.6ppm Noise, 4ppm INL, 10ppm Total Unadjusted Error, 200μA
LTC2404/LTC2408	4-/8-Channel, 24-Bit, No Latency ΔΣ ADC	0.3ppm Noise, 4ppm INL, 10ppm Total Unadjusted Error, 200μA
LTC2410	24-Bit, Fully Differential, No Latency ΔΣ ADC in SSOP-16	0.16ppm Noise, 2ppm INL, 3ppm Total Unadjusted Error, 200μA
LTC2411	24-Bit, Fully Differential, No Latency ΔΣ ADC in MS10	0.29ppm Noise, 2ppm INL, 3ppm Total Unadjusted Error, 200μA
LTC2415	24-Bit, Fully Differential, ΔΣ ADC	15Hz Output Rate at 60Hz Rejection, Pin Compatible with LTC2410
LTC2420	20-Bit, No Latency ΔΣ ADC in SO-8	1.2ppm Noise, 8ppm INL, Pin Compatible with LTC2400
LTC2424/LTC2428	4-/8-Channel, 20-Bit, No Latency ΔΣ ADC	1.2ppm Noise, 8ppm INL, Pin Compatible with LTC2404/LTC2408